INSTITUTO TECNOLÓGICO
Y DE ESTUDIOS SUPERIORES DE OCCIDENTE

Reconocimiento de validez oficial de estudios de nivel superior según acuerdo secretarial 15018, publicado en el Diario Oficial de la Federación el 29 de noviembre de 1976.

Departamento de Electrónica, Sistemas e Informática

DOCTORADO EN CIENCIAS DE LA INGENIERÍA

MODELADO SUSTITUTO INTEGRATIVO BNN-LHS Y ANÁLISIS TERMO-MECÁNICO-EM PARA LA CARACTERIZACIÓN MEJORADA DE FILTROS PASA BAJOS DE ALTA FRECUENCIA EN COMSOL

Tesis que para obtener el grado de

DOCTOR EN CIENCIAS DE LA INGENIERÍA

presenta: Jorge Dávalos Guzmán

Director de tesis: Dr. José Luis Chávez Hurtado

Co-director de tesis: Dr. Zabdiel Brito Brito

Tlaquepaque, Jalisco.
Diciembre de 2025

DOCTOR EN CIENCIAS DE LA INGENIERÍA (2025) ITESO, Tlaquepaque, Jal., México

TÍTULO: **Modelado Sustituto Integrativo BNN-LHS y Análisis Termo-Mecánico-EM para la Caracterización Mejorada de Filtros Pasa Bajos de Alta Frecuencia en COMSOL**

AUTOR: Jorge Dávalos Guzmán
Ingeniero en Comunicaciones y Electrónica (Universidad de Guadalajara, México)
Maestro en Ciencias en Electrónica y Computación (Universidad de Guadalajara, México)

DIRECTOR DE TESIS: José Luis Chávez Hurtado
Profesor del Departamento de Electrónica, Sistemas e Informática, ITESO
Ingeniero en Electrónica (ITESO, México)
Maestro en Diseño Electrónico (ITESO, México)
Maestro en Negocios y Estudios Económicos (Universidad de Guadalajara, México)
Doctor en Ciencias en Ingeniería (ITESO, México)
Member, IEEE

NÚMERO DE PÁGINAS: XCVIII

ITESO – The Jesuit University of Guadalajara

Department of Electronics, Systems, and Informatics

DOCTORAL PROGRAM IN ENGINEERING SCIENCES

INTEGRATIVE BNN-LHS SURROGATE MODELING AND THERMO-MECHANICAL-EM ANALYSIS FOR ENHANCED CHARACTERIZATION OF HIGH-FREQUENCY LOW-PASS FILTERS IN COMSOL

Thesis to obtain the degree of

DOCTOR IN ENGINEERING SCIENCES

Presents: Jorge Dávalos Guzmán

Thesis Director: Dr. José Luis Chávez Hurtado

Thesis Co-director: Dr. Zabdiel Brito-Brito

Tlaquepaque, Jalisco, Mexico
December 2025

PHD IN ENGINEERING SCIENCES (2025) ITESO, Tlaquepaque, Jal., Mexico

TITLE: **Integrative BNN-LHS Surrogate Modeling and Thermo-Mechanical-EM Analysis for Enhanced Characterization of High-Frequency Low-Pass Filters in COMSOL**

AUTHOR: Jorge Dávalos Guzmán
Bachelor of Engineering in Communications and Electronics (University of Guadalajara, Mexico)
Master of Science in Electronics and Computing (University of Guadalajara, Mexico)

THESIS DIRECTOR: José Luis Chávez Hurtado
Professor at the Department of Electronics, Systems, and Informatics, ITESO
Bachelor in Electronics Engineering (ITESO, Mexico)
Master in Electronic Design (ITESO, Mexico)
Master in Business and Economic Studies (University of Guadalajara, Mexico)
Doctor of Science in Engineering (ITESO, Mexico)
Senior Member, IEEE

NUMBER OF PAGES: XCVIII

A Dios

A mi familia

A mis compañeros y amigos

Resumen

Esta tesis presenta un enfoque integral para la simulación, modelado y optimización de estructuras de alta frecuencia (HF), enfocándose específicamente en filtros de microstrip de paso bajo. La investigación aprovecha las simulaciones COMSOL Multiphysics dirigidas por MATLAB, explorando varios esquemas de mallado para la microcinta, el sustrato y la caja de aire bajo 3 diferentes condiciones de temperatura, que van desde -80.15ºC, 19.85ºC y 119.85ºC. Esta investigación resalta las características clave del software y los pasos de modelado esenciales para simulaciones precisas.

El estudio introduce una metodología para desarrollar modelos sustitutos basados en electromagnetismo en el dominio de la frecuencia, considerando variaciones en las dimensiones físicas. Se comparan diversas técnicas de metamodelado, incluyendo redes neuronales de regresión generalizada (GRNN), Kriging y máquinas de vectores de soporte (SVM). COMSOL sirve como el modelo fino, generando datos de entrenamiento y prueba, mientras que MATLAB ayuda en el desarrollo de modelos sustitutos parametrizados. Los resultados indican una correspondencia razonable entre las respuestas del modelo fino y las de los modelos sustitutos, con precisión dependiendo de la técnica de metamodelado y del tamaño de la región de interés de entrenamiento.

Abordando los desafíos en el diseño de estructuras HF, especialmente al incorporar simulaciones multifísicas, esta investigación evalúa el rendimiento de diferentes técnicas de aprendizaje de redes neuronales artificiales (ANN): Levenberg-Marquardt, Bayesiana y Resiliente, para modelar un filtro de paso bajo de segundo orden multifísico. La ANN Bayesiana demuestra un rendimiento superior, modelando de manera eficiente y precisa la respuesta multifísica.

Además, se propone un marco avanzado de optimización térmica que integra una red neuronal bayesiana (BNN) con muestreo hipercubo latino (LHS) y variables de temperatura. Este marco refina el diseño de la malla para tener en cuenta los efectos térmicos, logrando simulaciones que reflejan de cerca las condiciones del mundo real. El estudio enfatiza el impacto de las variaciones de temperatura en el comportamiento electromagnético (EM), mejorando la precisión del modelado predictivo y proporcionando una metodología robusta para el desarrollo y optimización rápida de componentes EM en diversas condiciones ambientales.

Finalmente, la tesis presenta un enfoque transformador para el análisis EM utilizando una BNN informada por LHS dentro de las simulaciones COMSOL. Este método explora sistemáticamente el impacto de la variabilidad de las dimensiones físicas en el comportamiento del filtro, logrando una alta fidelidad en el modelado predictivo. Al analizar métricas como el Error Cuadrático Medio (MSE), el Error Máximo de Aprendizaje (MLE) y el Error Máximo de Prueba (MTE), la investigación demuestra que las estrategias específicas de variación y muestreo mejoran significativamente el rendimiento del modelo. El modelo desarrollado establece un nuevo estándar de fiabilidad y resistencia en el diseño y fabricación de componentes electrónicos.

En general, esta investigación contribuye al campo del diseño de estructuras HF al integrar técnicas de aprendizaje automático con la física computacional, potencialmente revolucionando el diseño y optimización de sistemas EM. Los hallazgos prometen reducciones significativas en los ciclos de desarrollo y mejoras en el rendimiento de dispositivos electrónicos, con amplias implicaciones para futuras investigaciones en telecomunicaciones, dispositivos médicos y otras aplicaciones que requieren un análisis EM preciso.

Summary

This thesis presents a comprehensive approach to the simulation, modeling, and optimization of high-frequency (HF) structures, specifically focusing on low-pass microstrip filters. The research leverages COMSOL Multiphysics simulations driven by MATLAB, exploring various meshing schemes for the microstrip, substrate, and air box under different temperature conditions, ranging from -80.15ºC, 19.85ºC and 119.85ºC. This investigation highlights key software features and modeling steps essential for accurate simulations.

The study introduces a methodology for developing electromagnetics-based surrogate models in the frequency domain, considering physical dimension variations. Various metamodeling techniques, including generalized regression neural networks (GRNN), Kriging, and support vector machines (SVM), are compared. COMSOL serves as the fine model simulator, generating training and testing data, while MATLAB aids in developing parameterized surrogate models. Results indicate a reasonable match between fine model responses and those of the surrogate models, with accuracy depending on the metamodeling technique and training region size.

Addressing the challenges in designing HF structures, especially when incorporating multiphysics simulations, this research evaluates the performance of different artificial neural network (ANN) learning techniques: Levenberg-Marquardt, Bayesian, and Resilient for modeling a multiphysical second-order low-pass filter. The Bayesian ANN demonstrates superior performance, efficiently and accurately modeling the multiphysical response.

Further, an advanced thermal optimization framework integrating a Bayesian Neural Network (BNN) with Latin Hypercube Sampling (LHS) and temperature variables is proposed. This framework refines mesh design to account for thermal effects, achieving simulations that closely mirror real-world conditions. The study emphasizes the impact of temperature variations on electromagnetic (EM) behavior, enhancing predictive modeling accuracy and providing a robust methodology for developing and optimizing EM components in various environmental conditions.

Finally, the thesis presents a transformative approach to EM analysis using a BNN informed by LHS within COMSOL simulations. This method systematically explores the impact

of physical dimension variability on filter behavior, achieving high fidelity in predictive modeling. By analyzing metrics such as Mean Squared Error (MSE), Maximum Learning Error (MLE), and Maximum Test Error (MTE), the research demonstrates that specific variation and sampling strategies significantly enhance model performance. The developed model sets a new benchmark for reliability and resilience in electronic component design and manufacturing.

Overall, this research contributes to the field of HF structure design by integrating machine learning techniques with computational physics, potentially revolutionizing EM system design and optimization. The findings promise significant reductions in development cycles and performance enhancements for electronic devices, with broad implications for future research in telecommunications, medical devices, and other applications requiring precise EM analysis.

Acknowledgements

The author wishes to express his deepest appreciation to Dr. José Luis Chávez Hurtado, Professor of the Department of Electronics, Systems, and Informatics at ITESO, for his unwavering encouragement, expert guidance, and insightful supervision as the primary director of this doctoral thesis throughout the course of this research.

The author also extends his heartfelt gratitude to Dr. Zabdiel Brito-Brito, Professor at the Centre Tecnològic de Telecomunicacions de Catalunya (CTTC), for his invaluable support and direction as the initial director during the early stages of this work, and later as the co-director, providing continued guidance and expertise.

The author offers his gratitude to Dr. José Ernesto Rayas Sanchez for his support in the early stage of the development of this work.

A very special acknowledgment to Dra. Gabriela Calvario-Sánchez, whose remarkable leadership and unwavering support ensured that I always had the resources and motivation to keep moving forward. Special thanks are also due to Dra. Aurea Edna Moreno Mojica, Dr. Ramon Osvaldo Guardado Medina, Riemann Ruiz Cruz and Dr. Anuar Benjamín Beltrán González, members of the Ph.D. Thesis Committee, for their insightful evaluation, constructive feedback, and thoughtful suggestions.

The author has greatly benefited from working with COMSOL Multiphysics developed by COMSOL Inc. and MATLAB developed by The MathWorks Inc.

It is the author's pleasure to acknowledge fruitful collaboration and stimulating discussions with his colleague of CAECAS research group at ITESO – The Jesuit University of Guadalajara: Felipe de Jesus Leal Romo, Andres Viveros Wacher, Jesus Gomez Lopez, and Francisco Rangel Patiño.

The author gratefully acknowledges the financial assistance through a scholarship granted by the *Consejo Nacional de Ciencia y Tecnología* (CONACYT), Mexican Government, as well as the financial support provided by Intel Corporation during the years of his doctoral studies, through a CAECAS research project funded by Intel Mexico.

Finally, special thanks are due to my family, for their understanding, patience, and continuous loving support.

Contenido

Contents

List of Figures

List of Tables

Introduction

The escalating complexity and performance requirements of high-frequency (HF) structures in various engineering domains necessitate sophisticated design and optimization techniques. Traditional electromagnetic (EM) simulation methods, while highly accurate, are often prohibitively time-consuming and computationally expensive. This doctoral dissertation addresses these challenges by developing advanced surrogate modeling techniques and incorporating multiphysical considerations to enhance the efficiency and accuracy of HF structure design processes.

One of the primaries focuses of this research is the development and application of surrogate models. Surrogate models offer a computationally efficient alternative to direct EM simulations by approximating the behavior of HF structures. This dissertation explores several surrogate modeling techniques, including generalized regression neural networks (GRNN), Kriging, support vector machines (SVM), and polynomial functions. These techniques are applied to model low-pass microstrip filters in the frequency domain, using COMSOL Multiphysics as the fine model simulator and MATLAB for data generation and model development. The results demonstrate that Kriging provides the best performance among the compared techniques, with a reasonable match between the fine model responses and the surrogate models developed.

The research also integrates multiphysical effects into the surrogate modeling process. HF structures are often subjected to thermal and mechanical stresses, which can significantly influence their EM behavior. Traditional modeling approaches that neglect these effects may lead to suboptimal designs. This dissertation proposes methodologies that incorporate thermal and mechanical interactions into the surrogate models, providing a more comprehensive understanding of HF structure behavior under real-world conditions. For instance, the study demonstrates how temperature variations can affect the deformation of a microstrip low-pass filter, highlighting the importance of considering multiphysical effects in EM simulations.

To further enhance optimization efficiency, this dissertation investigates the use of Bayesian Neural Networks (BNNs) combined with Latin Hypercube Sampling (LHS). This approach allows for the precise modeling of low-pass filters, considering temperature variables and other multiphysical factors. The integration of BNNs with LHS has proven instrumental in

capturing the subtleties of EM behavior, offering significant improvements in simulation accuracy and efficiency. The results indicate that BNNs, particularly when enhanced with LHS, can generalize effectively from diverse datasets to unseen conditions, marking a paradigm shift towards rapid, data-driven filter optimization.

Additionally, the research explores the use of Artificial Neural Networks (ANNs) for modeling the multiphysical response of HF structures. A comparison of three ANN learning techniques Levenberg-Marquardt, Bayesian, and Resilient reveals that Bayesian ANN provides the best performance for accurately modeling the EM responses of a multi-physics second-order low-pass filter implemented in COMSOL. These findings underscore the potential of ANNs in developing fast and accurate surrogate models for complex HF structures.

The organization of this doctoral dissertation is as follows:

Chapter 1 reviews previous methodologies in electromagnetics-based surrogate modeling and presents the development and simulation of a microstrip low-pass filter using COMSOL Multiphysics driven by MATLAB. It details the selection of meshing schemes and the simulation process under 3 varying temperatures from -80.15ºC, 19.85ºC and 119.85ºC.

Chapter 2 discusses the development of electromagnetics-based surrogate models for low-pass microstrip filters, considering physical dimension variations. Several metamodeling techniques, including GRNN, Kriging, and SVM, are compared. The chapter showcases the performance of these surrogate models in relation to the fine model responses, considering the size of the training region of interest.

Chapter 3 addresses the challenges of designing HF structures under multiphysical conditions involving thermal and mechanical interactions with electromagnetic responses. It evaluates the performance of three ANN learning techniques Levenberg-Marquardt, Bayesian, and Resilient for modeling a multi-physics second-order low-pass filter in COMSOL. Results indicate that the Bayesian ANN technique offers the best performance for accurately modeling the multi-physical response of HF structures.

Chapter 4 proposes an advanced thermal optimization framework for predictive low-pass filter modeling, integrating BNNs enhanced with LHS and temperature variables. The chapter emphasizes refining mesh design to account for thermal effects and simulates real-world operational conditions with precision.

Chapter 5 introduces a transformative approach to EM analysis of coarse low-pass filter

models using an integrative BNN informed by LHS within COMSOL simulations. This chapter systematically examines the impact of physical dimension variability on filter behavior, evaluating model accuracy through metrics such as Mean Squared Error (MSE), Maximum Learning Error (MLE), and Maximum Test Error (MTE).

The general conclusions summarize the significant insights and overall efficacy of the proposed methodologies in modeling and optimizing HF structures. Additionally, future research directions are suggested, building on the foundations laid by this dissertation.

Finally, Appendix A lists the fourteen internal research reports generated throughout the doctoral studies, while Appendix B presents a compilation of the conference and journal papers derived from this research, in which the doctoral candidate served as the primary author.

1. Multiphysics Simulation of a Microstrip Low-Pass Filter in COMSOL using a MATLAB Driver

To know the multiphysics effects of microstrip circuits when running at high frequencies has become a very important study trending field. Especially when dealing when performance and EM optimization [Estrada-Arámbula-11], [Vargas-Chávez-11], [Rayas-Sánchez-12a], [Rayas-Sánchez-12b], [Gutiérrez-Ayala-09], [Rayas-Sánchez-12c].

In this chapter a microstrip low-pass band filter is analyzed using COMSOL Multiphysics. The filter described was widely studied and optimized in [Rayas-Sánchez-12b], where Sonnet was employed for its EM analysis. Now, we perform a different approach by modelling and driving a multiphysics simulation (thermal, mechanical, and electromagnetic analysis) using a MATLAB driver to exploit COMSOL feature called MATLAB Live Link plug in.

1.1. COMSOL Features Using MATLAB

COMSOL[1] Multiphysics offers a large and well-managed interface to MATLAB[2] which is called MATLAB Live Link that allows the user to perform a wide variety of data pre-processing and post-processing. COMSOL has tremendous modeling capabilities that allow the user and easy geometry definition, material properties selection and physics modeling. These settings are not hardwired and can be manually configured in the solver settings or under a MATLAB driver to tune the performance for a specific problem.

Usage of drivers to manage solvers and other computationally intense algorithms can be fully parallelized to make better use of multicore computing as well as for large parametric sweeps.

1.2. Creation and Configuration of the COMSOL Model

[1] COMSOL Multiphysics version 5.3a 2018, COMSOL AB, Tegnérgatan 23, SE-111 40 Stockholm, Sweden.
[2] Matlab R2017a, Version 9.2.0.5, the MathWorks, Inc., 3 Apple Hill Drive, Natick MA 01760-2098, 2018.

The microstrip model implemented on this chapter is shown in Fig. 1.1,

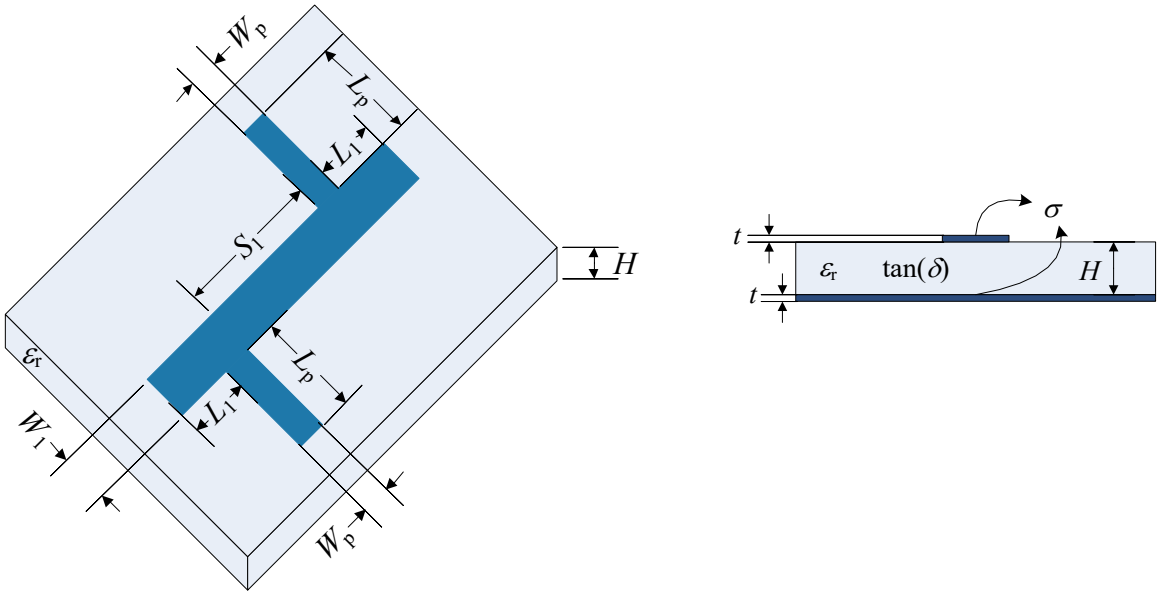

Fig. 1.1 Low-pass microstrip filter geometry taken from [Rayas-Sánchez-12b], to illustrate the physical dimensions of the circuit.

the duroid substrate used for the structure has a thickness of H=0.794 mm and a dielectric constant of ε_r = 2.2 with a loss tangent tan(δ) = 0. The physical design dimensions are W_1 = 2.191, L_1= 5.079 (mm), W_p= 5.062 (mm), S_1= 5.052 (mm), t = 0, and H_{air}= 7.94. We neglected losses for metals and dielectric tan (δ) = 0, as well for Γ = ∞. The full list of the parameters used on this chapter was taken from [Rayas-Sánchez-12a].

We defined the additional parameters in COMSOL for the physical structure, and we briefly mention the main ones. Young's modulus and Poisson's ratio property definitions which are for metals and dielectric materials. We also used a perfect electric conductor for the microstrip and the walls of the air box, and ground plane horizontally lumped ports for the filter under the EM definitions of the model.

For the meshing scheme we used the free-tetrahedral with three different sizes [Jian-Ming-14]. For the microstrip structure we defined an edge meshing, as shown in Fig. 1.2.

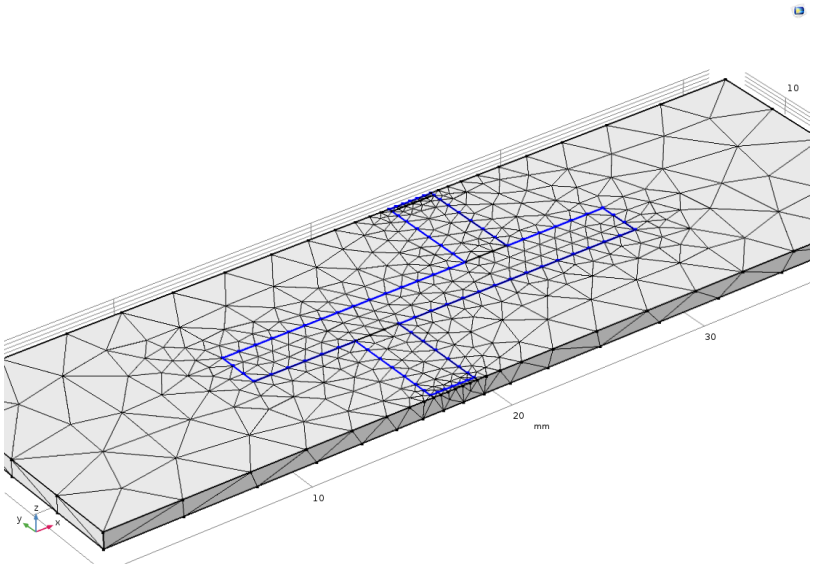

Fig. 1.2 Meshing used inside the microstrip area as simulated in COMSOL.

These element sizes can be controlled defining *MinMcsl* and *MaxMcsl* parameters. For the ports we defined a boundary meshing as shown in Fig. 1.3.

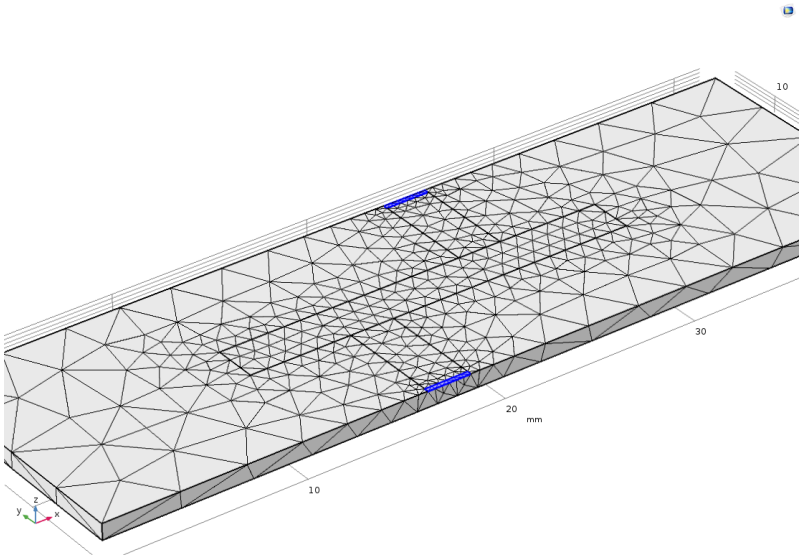

Fig. 1.3 Meshing used in the ports as simulated in COMSOL.

In this case, the *MinPort* and *MaxPort* parameters were used to fix the element size at the ports. Finally, a global meshing was defined for the rest of the structure. We used the *MinGlobal* and *MaxGlobal* parameters to fix the sizes of said elements.

1.3. MATLAB Driver

To perform a brief parametric sweep, we used the COMSOL tool called MATLAB LiveLink to run our custom MATLAB code (driver). This code includes a predefined function, *mphload*, which allows us to load the COMSOL project into MATLAB. Another key function used in this process is *model.param.set*, which enables us to set the values of all variables predefined in the COMSOL project. After setting the desired parameter values, we run the simulation using the function *model.sol().runAll*.

Additionally, the function *mphglobal* allows extract data from COMSOL (*e.g.*, S-parameters, frequency, etc.). Said MATLAB driver also extracts plots from the COMSOL model using the *mph.plot* function. This driver is documented in [Dávalos-Guzmán-19a].

Finally, we can identify 3 main stages needed when building a MATLAB driver to run simulations in COMSOL: 1) setting all the parameter values; 2) transferring parameter values to COMSOL; 3) running the simulation in COMSOL from MATLAB Live Link.

1.4. Temperature Dependence Simulation

The MATLAB driver was set up with ambient temperature as a global design parameter to run the Multiphysics analysis with thermal dependency across the entire simulation domain. This means the parameter affects not only the dielectric materials and the microstrip structure but also the surrounding air box volume. In this way, the results can be compared on a step-by-step basis as the temperature varies in the plot.

In this chapter, we performed a parametric temperature sweep at –80.15 °C, 19.85 °C, and 119.85 °C using a MATLAB-driven COMSOL simulation. These values were arbitrarily selected to span extreme cold, ambient, and high-temperature conditions, enabling a broad analysis of thermal effects. Each simulation took ~15 minutes on a 3.4 GHz CPU with 16 GB RAM. Results showed that at –80.15 °C, cold air accumulates near the top of the air box, as illustrated in Fig. 1.4.

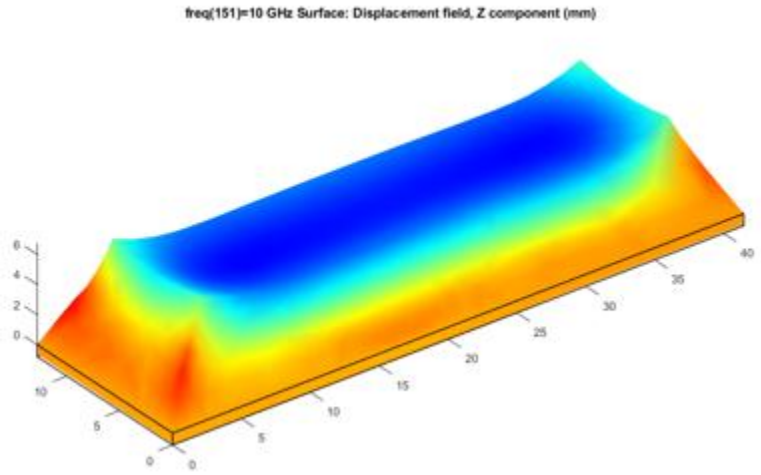

Fig. 1.4. Solid stress deformation of the air box from the low-pass filter at -80.15°C.

With an ambient temperature of 19.85ºC, the observed effect is also null as in Figs. 1.5.

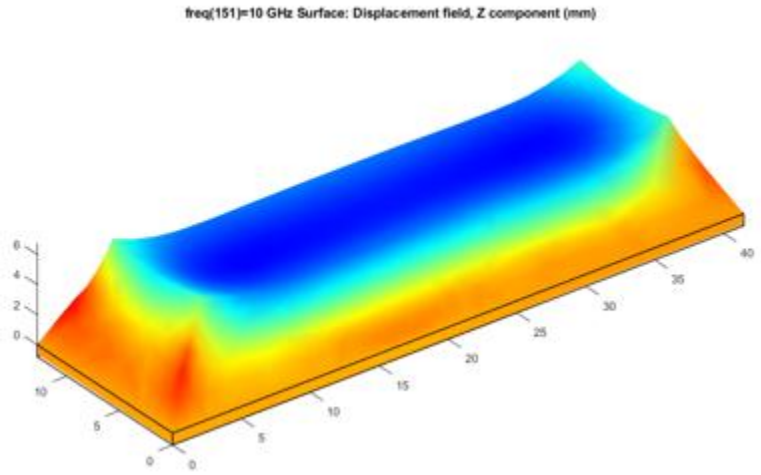

Fig. 1.5. Solid stress of the complete air box from the low-pass filter at 19.85°C.

An interesting phenomenon happens as the temperature increases, as shown in Fig. 1.6,

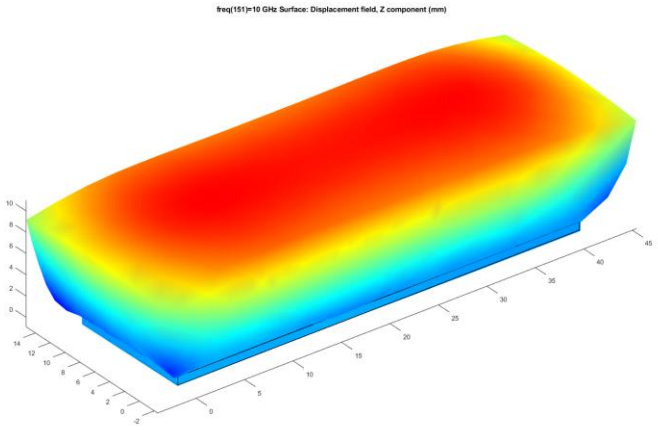

Fig. 1.6. Solid stress deformation of the air box from the low-pass filter at 119.85°C.

The air box gets modified because the air contained in box expands. We added some other views of a substrate stress modification suffered in the 3 temperatures; these are shown in Figs. 1.7 to 1.9.

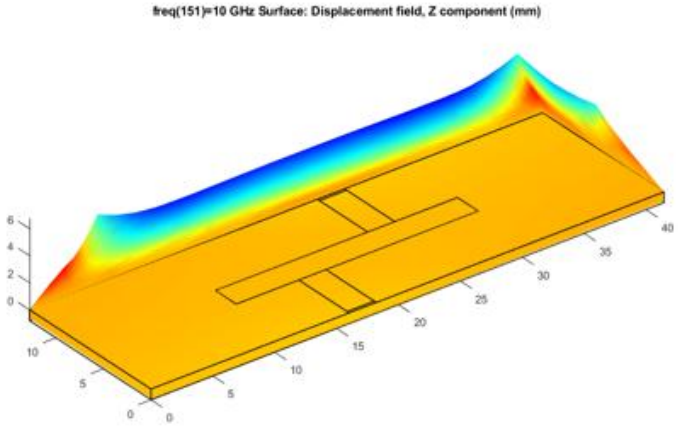

Fig. 1.7. Mechanical deformation of the substrate from the low-pass filter at -80.15°C.

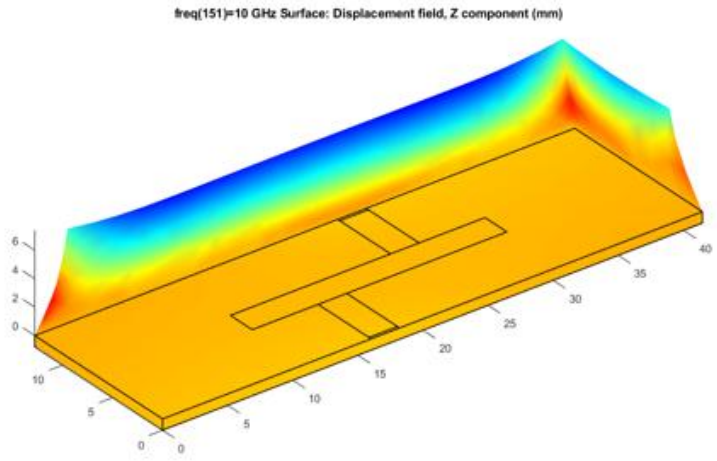

Fig. 1.8. Mechanical deformation of the substrate from the low-pass filter at 19.85°C.

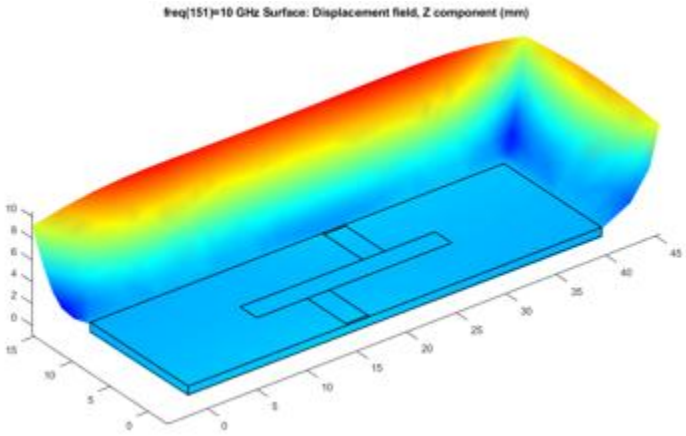

Fig. 1.9. Mechanical deformation of the substrate from the low-pass filter at 119.85°C

. The S-parameters $|S_{11}|$ and $|S_{21}|$ respectively represent the input reflection coefficient and the forward transmission coefficient of the low-pass filter. In Fig. 1.10, $|S_{11}|$ indicates how much of the signal is reflected at the input port, while $|S_{21}|$ shows how much of the signal is transmitted through the filter to the output. Ideally, a low-pass filter should present low $|S_{11}|$ and high $|S_{21}|$ values in the passband (low frequencies), and the inverse behavior in the stopband (high frequencies). The figure illustrates how temperature variations slightly shift the filter's cutoff frequency and affect the magnitude of both parameters, with higher temperatures showing a small detuning effect. These variations suggest a temperature-induced shift in the effective dielectric properties of the structure

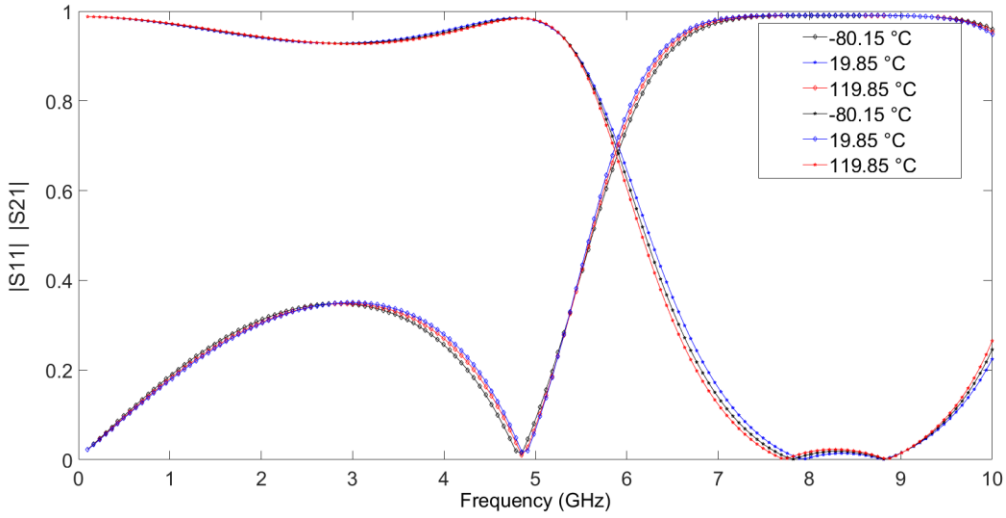

Fig. 1.10. S Parameters $|S_{11}|$ and $|S_{21}|$ of a temperature sweep from -80.15°C to 119.85°C for the low-pass microstrip filter.

1.5. Conclusions

In this chapter a way to perform a COMSOL Multiphysics simulation of a microstrip low-pass filter driven by MATLAB is presented. We configured the driver to perform a sweep at 3 different temperatures. We implemented different meshing schemes for the microstrip on the Multiphysics simulation. Finally, we present the results where it can be seen clearly the deformation of the air box caused by the temperature that expanded and contracted of the inner air.

2. Electromagnetic Surrogate Modeling of a Microstrip Low-Pass Filter

The usage of surrogate models represents a significant computing time reduction when performing simulations. Some of the most common surrogate modeling techniques are generalized regression neural networks (GRNN) [Song-20], Kriging [Xia-14], and support vector machines (SVM) [Khandelwal-15]. These techniques have been employed, for instance, to approximate the EM performance of high-frequency structures, such as substrate integrated waveguide (SIW) interconnects, planar inverted F antennas (PIFA), and via-stripline-via transitions [Chávez-Hurtado-15b]. An initial surrogate modeling approach to approximate the multi-physical performance of a simple microstrip line is reported in [Chávez-Hurtado-16c].

COMSOL simulations of a low-pass microstrip filter considering only its electromagnetic performance in frequency domain are realized in this work. The corresponding COMSOL model is considered here as a fine model, given its high accuracy and relatively high computational cost. In future work, this fine model will be enhanced by implementing subsequent steps to incorporate thermal and mechanical behaviors, to then develop a multi-physics surrogate model.

The low-pass microstrip filter employed in this chapter uses several parameterized design dimensions. A variation of its physical design dimensions was performed, and the corresponding EM simulations were realized using COMSOL driven from MATLAB, obtaining the corresponding S-parameters. These responses and input variables are used to generate training and test data to develop several surrogate models. Once the surrogate models are trained, their responses are compared with those of the original EM model, measuring the corresponding training and testing errors.

2.1. Main Surrogate Modeling Purpose and Terminology

Let $\boldsymbol{R}_f \in \Re^p$ denote the fine model EM response sampled at p frequency points. Vector $\boldsymbol{x} \in \Re^n$ contains the selected n design variables of the structure. Our main purpose is to develop a surrogate model $\boldsymbol{R}_s(\boldsymbol{x})$ whose responses match those of the original fine model within some training

region of interest in the design space.

The size of the training region is defined by vector $\boldsymbol{\tau} \in \Re^n$, which contains the relative deviation for each design variable with respect to a reference design $\boldsymbol{x}^{(0)}$. To train the surrogate model we use L learning base points. The training or learning errors are measured at the j-th learning base point for the k-th simulated frequency point, with $j = 1, 2\ldots, L$, and $k = 1, 2, \ldots p$. To measure the generalization error of the surrogate models, we use a set of T testing base points not used during training but within the same modeling region.

2.2. Surrogate Modeling Example

2.2.1 Microstrip Filter to be Modeled

Consider the low-pass microstrip filter shown in Fig. 2.1.

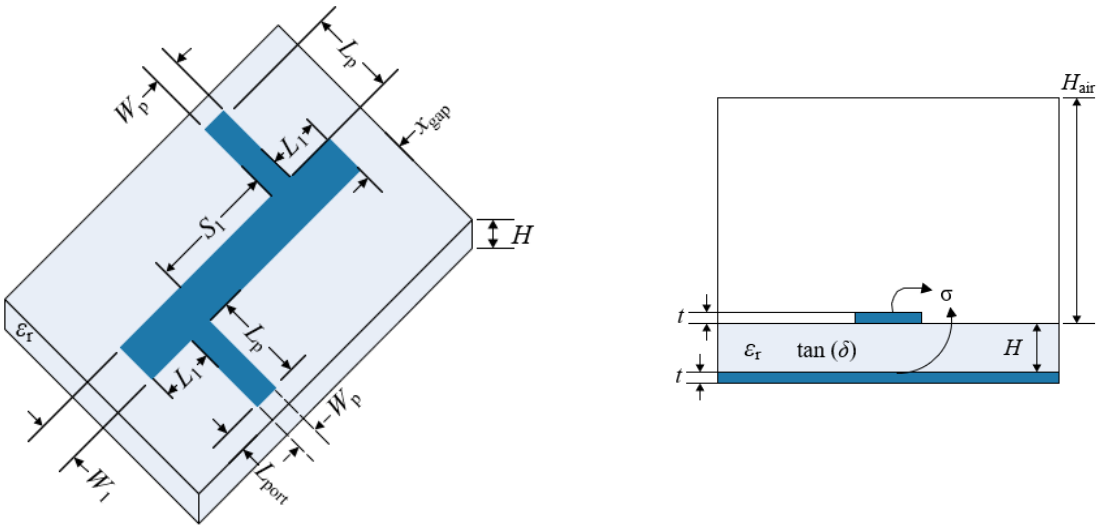

Fig. 2.1. Geometry of the low-pass microstrip filter. Figure taken from [Rayas-Sánchez-12d], to illustrate the physical dimensions of the circuit.

It uses a dielectric substrate whose height is H = 0.794 mm with a relative dielectric constant ε_r = 2.2 and a dielectric loss tangent $\tan(\delta)$ = 0.0025. The feed-line width is defined as W_p = 2.191 mm to achieve 50-Ω input/output lines. The selected feed-line length is L_p = 5.079 mm. The reference design $\boldsymbol{x}^{(0)}$ of this filter uses W_1 = 2.467 mm, S_1 = 5.053 mm, and L_1= 5.062 mm

(see Fig. 2.1). All metallic traces are defined as copper with a thickness t = 0.17 μm [Rayas-Sánchez-12e].

The filter structure is implemented in COMSOL using a simulation bounding box shown in Fig. 2.1, where $\boldsymbol{x}_{\text{gap}}$ = 10.95 mm is the lateral separation from the box edge and H_{air} = 7.94 mm is the air layer height. Horizontal lumped ports were used, with a port length L_{port} = 0.21 mm. We follow the same meshing scheme proposed in [Chávez-Hurtado-16d].

To develop the surrogate model, we define $\boldsymbol{x} = [W_1 \;\; S_1 \;\; L_1]^{\text{T}}$ and use $\boldsymbol{x}^{(0)} = [2.467 \;\; 5.053 \;\; 5.062]^{\text{T}}$ (mm) as the central base point over a region of interest defined by a relative perturbation size $\tau \in \Re$, equally applied to all the elements in $\boldsymbol{x}$. We define different training region sizes by arbitrary selecting τ as 5%, 10%, 15%, and 20%. All the EM simulations implemented in COMSOL in this report were performed at a fixed temperature T = 293.15 K (20 °C).

2.2.2 Loading the Input Data and Training the Surrogate Models

To train the surrogate models we use 5 uniformly distributed points for each element of $\boldsymbol{x}$, resulting in a set of 125 learning base points (5^3). The responses of interest are $|S_{11}|$ and $|S_{21}|$ for a frequency range of 0.1 GHz to 10 GHz, using p = 50 frequency points per frequency sweep. We use as target the EM responses obtained from COMSOL.

The MATLAB commands used on the learning modeling process for the SVM, GRNN and Kriging are fitrsvm, newgrnn, and fitrgp, respectively. To get the response predictions and calculate the error measurements for SVM, GRNN, and Kriging, we use the following MATLAB commands:

```
predict(mdl_SVM{freq},input(cont,:))
sim(mdl_GRNN{freq},input(cont,:)
predict(mdl_Kriging{freq},input(cont,:))
```

where cont works under a for cycle within a range of 1 to 125 learning data points, {freq} are the 50 frequency points equally distributed from 0.1 GHz to 10 GHz. The function names assigned to train the model with SVM, with GRNN, and with Krigging, are mdl_SVM, mdl_GRNN, and mdl_Kriging, respectively. We use functions predict and sim to execute the performance learning process and to obtain the generalization performance errors, respectively.

2.2.3 Testing the Surrogate Models

An arbitrary set of 100 random base points is used to calculate the maximum absolute testing error at each frequency point, stored in vector $\boldsymbol{\epsilon}_T \in \Re^p$, and the maximum absolute testing error in the complete frequency sweep, denoted as ϵ_{Tmax}. The maximum absolute errors of the resultant surrogate models for the responses of interest at each training region size are summarized in Table 2.1,

TABLE 2.1
MAXIMUM ABSOLUTE GENERALIZATION ERROR FOR ALL SIMULATED FREQUENCY POINTS FOR THE LOW-PASS MICROSTRIP FILTER

Model	ϵ_{Tmax} for $\lvert S_{11}\rvert$				ϵ_{Tmax} for $\lvert S_{21}\rvert$			
	$\tau = 5\%$	$\tau = 10\%$	$\tau = 15\%$	$\tau = 20\%$	$\tau = 5\%$	$\tau = 10\%$	$\tau = 15\%$	$\tau = 20\%$
SVM	0.1718	0.1368	0.3064	0.3803	0.1479	0.1204	0.2088	0.2776
Kriging	0.1918	0.1615	0.1842	0.1536	0.1446	0.0978	0.1068	0.0943
GRNN	0.1419	0.1808	0.3271	0.3778	0.1220	0.1458	0.2359	0.2622

It is seen from Table 2.1 that, when modeling $|S_{11}|$, the best surrogates are: GRNN for $\tau = 5\%$, SVM for $\tau = 10\%$, and Kriging for $\tau = 15\%$ and 20%. When modeling $|S_{21}|$ the best surrogates are: GRNN for $\tau = 5\%$, and Kriging for $\tau = 10\%$, 15%, and 20%. These results indicate that Kriging has better performance in large regions and GRNN outperforms Kriging when the region of interest is very small.

It is observed that with some surrogate models the generalization error is larger in small training regions and smaller in large training regions. Two independent experiments were performed to corroborate this by using the same methodology and achieved the same results. This atypical behavior might have been caused due to the arbitrary selection of the testing points. Finally, Fig. 2.2 shows a graphical comparison of the errors of all surrogate models with respect to frequency.

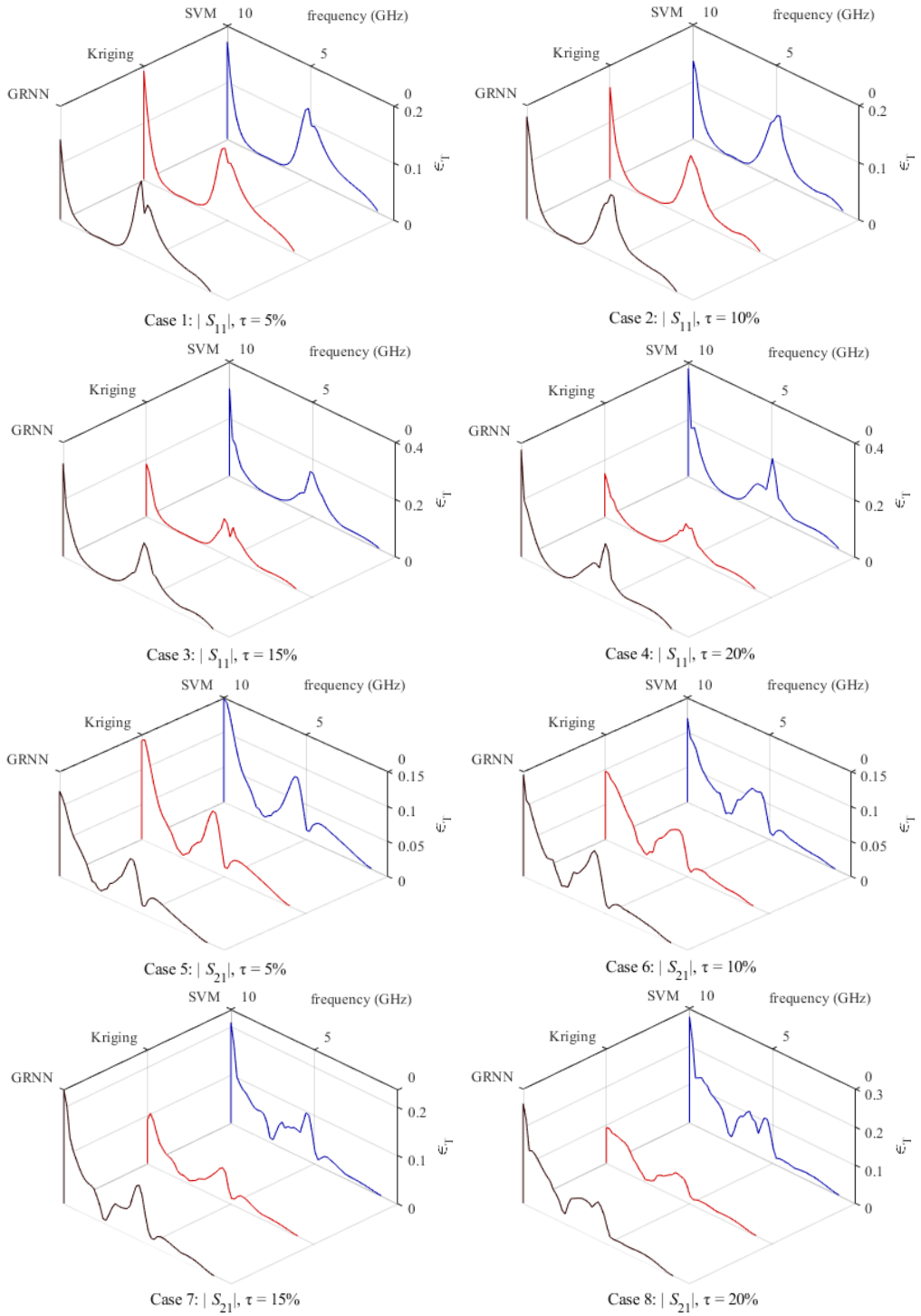

Fig. 2.2 Graphical representation to compare the testing errors of the GRNN, Kriging, and SVM surrogate models in the frequency range of interest.

2.3. Conclusions

In this chapter we presented a methodology to develop an electromagnetics-based surrogate model of a low-pass microstrip filter in the frequency domain and with physical dimension variations. We compared the generalized regression neural networks (GRNN), Kriging, and support vector machines (SVM). A reasonable match between the fine model responses and those of the parameterized surrogate models developed were obtained. Varying accuracies depending on the surrogate modeling technique employed and the size of the training region of interest were observed. Results after applying the surrogate models indicate that the best modeling performance is achieved by Kriging for this problem.

3. Neural Network Learning Techniques Comparison for a Multiphysics Second Order Low-Pass Filter

Artificial neural networks (ANNs) have been extensively used to develop fast and accurate surrogate models of high-frequency structures characterized by computationally expensive electromagnetic (EM) simulations [More-77], [Rumelhart-86]. EM efficient trained artificial neural network (EM-ANN) allows the EM circuit design simulation and optimization to be fast and accurate [Waremstein-19], [Zhang-20], [Zhang-19].

One of the key advantages of combining multiphysics simulations and ANNs is the ability of these last to handle non-linear optimization problems [Levenberg-44]. Different learning techniques can be applied to develop ANN, such as the Levenberg-Marquardt ANN, Resilient ANN and Bayesian ANN. The Levenberg-Marquardt method is a trust region algorithm which aims to find a minimum of a function over a space of parameters. The trust region of the objective is modeled by a quadratic function and when the adequate fit is found the region is expanded [Levenberg-44], [Marquardt-63].

The resilient backpropagation (BP) method is based on gradients. Like Manhattan update rule, resilient BP algorithm uses only the sign of the gradient to determine a weight delta. Also, it maintains separate weight deltas for each weight and bias and adapts them during training [Prasad-13]. The Bayesian ANN uses statistical distributions to quantify uncertainty introduced by models in terms of outputs and weights. Compared to standard ANN, Bayesian ANN focuses on marginalization instead of optimization, the estimate of parameters is done by the maximum posteriori instead of maximum likelihood estimators. The optimal value is found by using Markov Chain Monte Carlo, Variational Interference or Normalizing Flows instead of gradient descent [Khan-20], [Jafari-10].

In this chapter, a comparison of the three learning methods is done to determine the best ANN surrogate model for a second order multi-physics low pass filter implemented in COMSOL. The multi-physics simulation considers the electromagnetic, thermal, and mechanical response of the structure under study.

3.1. Multi-Physical Circuit

The microstrip filter used in this chapter is modeled in COMSOL and consists of a low pass microstrip filter exhibiting multi-physical behavior (EM, thermal, and mechanical). Multi-physics simulations are very high time consuming and computationally expensive. The corresponding model for the low pass filter is shown in Fig. 3.1.

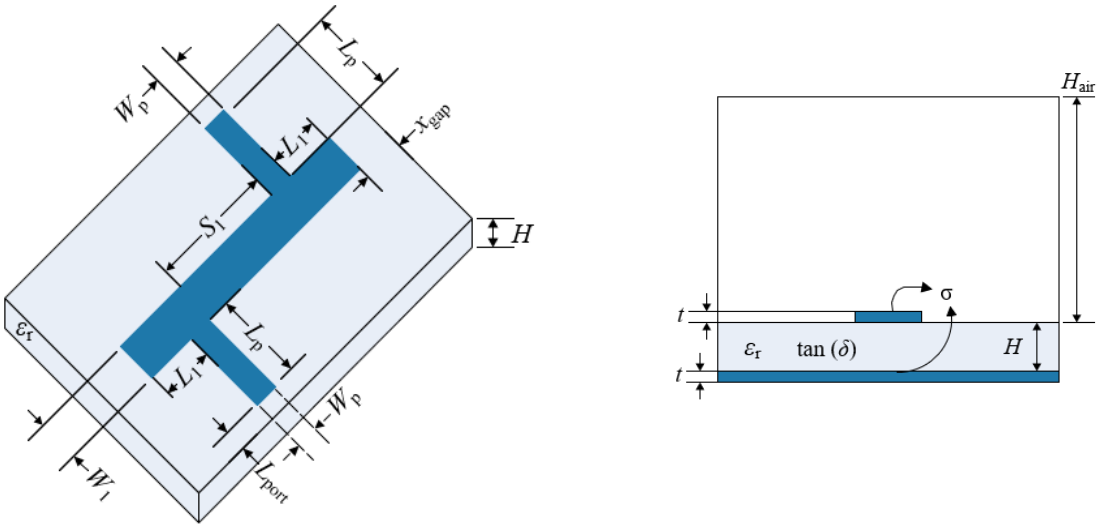

Fig. 3.1. Geometry of the low-pass microstrip filter. Figure taken from [Rayas-Sánchez-12d], to illustrate the physical dimensions of the circuit.

The filter structure is implemented in COMSOL using a dielectric substrate with a height H = 0.794 mm, a relative dielectric constant ε_r = 2.2 and a dielectric loss tangent tan(δ) = 0.0025. The feed-line width is defined as W_p = 2.191 mm to achieve 50-Ω input/output lines. The selected feed-line length for the filter is L_p = 5.079 mm, W_1 = 2.467 mm, S_1 = 5.053 mm, and L_1= 5.062 mm. All metallic traces are defined as copper with a thickness t = 0.17 μm [Dávalos-Guzmán-19b].

To be properly simulated, a simulation bounding box is required, with $\boldsymbol{x}_{gap}$ = 10.95 mm defined as the lateral separation from the box edge and H_{air} = 7.94 mm defined as the air layer height. Horizontal lumped ports were used with a port length Lport = 0.21 mm. For the structure meshing we follow the scheme proposed in [Rayas-Sánchez-12b]. Each multi-physics simulation takes approximately 20 minutes using a personal computer with a core i7 processor and 16GB RAM.

3.2. ANN Surrogate Model

The development of a neural network model includes the generation of representative training data within the region of interest (called learning base points) and the selection of the network topology and training techniques. Once trained, the ANN model performance is measured by using random testing base points within the region of interest.

The multilayer perceptron (MLP) neural network is appropriate for this functional mapping problem [Zhang-13]. We used a 3-layer perceptron (3LP) to implement our neuro-model, with n inputs, h hidden neurons, and m outputs. The required complexity of the ANN, determined by h, depends on the generalization performance for a given set of testing data [Cybenko-89].

To obtain the best ANN surrogate model, three different learning algorithms were implemented: Levenberg-Marquardt BP, resilient BP, and Bayesian Regularization.

To train and generate the ANN surrogate models, we used the Neural Network toolbox included in MATLAB. The training functions were specified as follows:

- 'trainlm' for Levenberg–Marquardt BP
- 'trainrp' for Resilient BP
- 'trainbr' for Bayesian Regularization

It is important to mention that during the use of these training functions, no hyperparameter tuning was performed; the models were trained using MATLAB's default settings for each algorithm. For further reference, we added Table I into the Appendix to summarize the ANN training algorithms and default parameters used in MATLAB's neural network toolbox. These parameters were not modified during training and serve as the default configuration for each respective algorithm.

A total of 158,100 data samples were generated for training, validation, and internal testing of the ANN surrogate models. These samples were produced by simulating 100 geometric variation sets, each evaluated across 31 discrete temperature values ranging from –50 °C to 100 °C in 5 °C steps, and 51 frequency points, resulting in, 100 sets × 31 temperatures × 51 frequency points = 158,100 base points.

From this dataset, 80% (126,480 samples) were used for training, 10% (15,810 samples) for validation, and 10% (15,810 samples) for internal testing. In addition, a separate set of 2,550 samples was generated using 10 intermediate temperature values not included in the training

sweep. This external testing dataset was created specifically to assess the model's generalization capabilities under unseen thermal conditions.

To assess the performance of the ANN models, the following error metrics were calculated: Mean Squared Error (MSE) the average of the squared differences between the ANN output and the circuit response at the training points; Maximum Learning Error (MLE) the maximum difference between the ANN and the circuit response over the training set; and Maximum Testing Error (MTE) the maximum deviation observed between the ANN and the circuit response on the unseen (random) testing points.

The final number of hidden neurons for each training algorithm was determined following the guideline from [Hornik-89], which suggests stopping at the point where the testing error no longer improves relative to the training error.

3.3. ANN Modeling Results

For developing the ANN surrogate models, we generate 50 learning base points uniformly distributed from -50 °C to 100 °C. We also use inputs 51 uniformly distributed frequency points, from 0.1 GHz to 4 GHz. The circuit response $|S_{21}|$ is used as the target for the ANN model. To measure the generalization performance, we generate 10 random temperature testing points within the temperature range. For each training algorithm we developed 20 ANN models and selected the model with the best generalization performance.

Corresponding MSE, MLE, and MTE for the three learning techniques can be seen in Fig. 3.2,

Fig. 3.2. Corresponding MSE, MLE, and MTE for the Bayesian, Resilient, and Levenberg Marquardt ANN using 20 trials.

The number of hidden neurons selected for the best ANN models can be seen in Fig. 3.3 that illustrates the behavior of the training and testing errors denoted as $\log_{10}(e_L)$ and $\log_{10}(e_T)$, respectively as a function of the number of hidden neurons h, for each ANN training algorithm: Bayesian Regularization**,** Resilient Backpropagation, and Levenberg–Marquardt**.** The plotted errors correspond to the base-10 logarithm of the MSE values for both training and testing datasets. These metrics were used to evaluate the model's ability to fit the training data and generalize to unseen data, respectively.

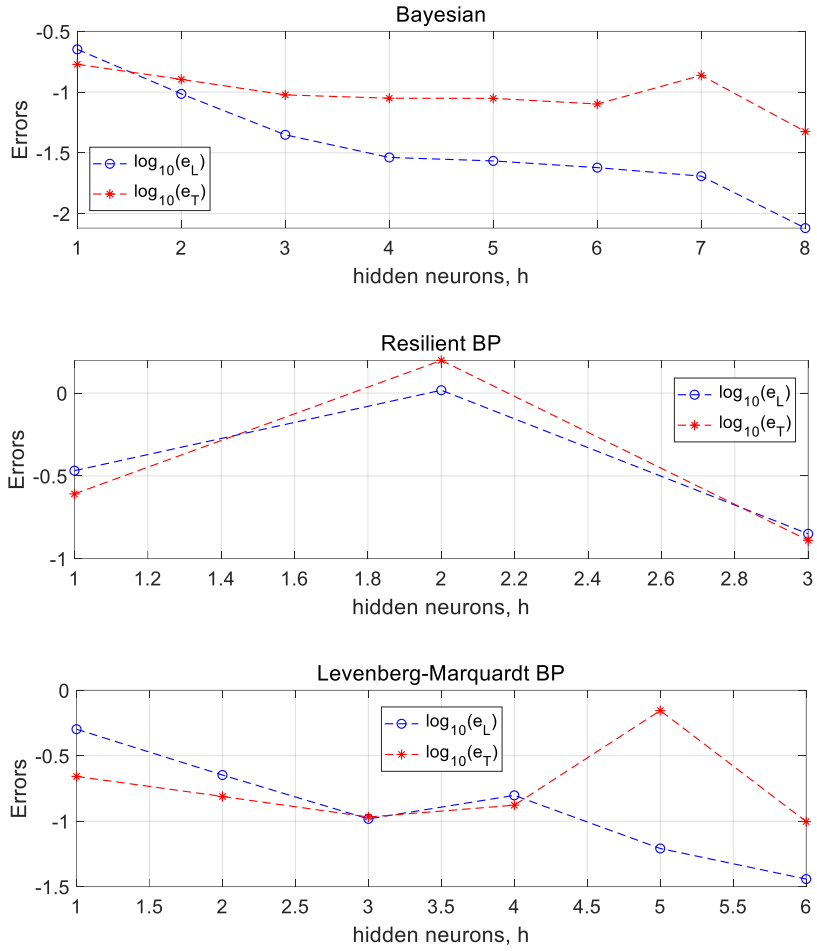

Fig. 3.3 Plotted errors corresponding to the base-10 logarithm of the MSE values for both training $\log_{10}(e_T)$ in red lane, testing datasets $\log_{10}(e_L)$ in blue lane and the corresponding number of hidden neurons h for each ANN training algorithm.

The selection of the optimal number of hidden neurons for each algorithm was guided by observing the point where the testing error no longer decreases significantly or starts to increase (i.e., the point where overfitting begins). This is consistent with the guideline in [Hornik–89], which recommends stopping at the minimum generalization error.

For Bayesian Regularization, the optimal number of hidden neurons was selected as $h = 1$, where both training and testing errors reached their lowest values, and the curves remained stable, indicating excellent generalization without overfitting.

For Resilient BP, the best performance was observed at h=1. Although 2 neurons had lower training errors, the corresponding testing error was higher, suggesting overfitting. At $h = 3$, both as $\log_{10}(e_L)$ achieved a good balance with minimal error gap.

For Levenberg–Marquardt BP, the minimum testing error occurred at $h = 4$. Lower values

of h reduced the training error but led to a slight increase in testing errors beyond this point.

According to the results obtained, the best generalization performance error is achieved by the Bayesian regularization technique. The corresponding results for the 10 random temperature conditions at selected testing base points are shown in Fig. 3.4. A strong agreement is observed between the responses of the Bayesian ANN and the COMSOL model.

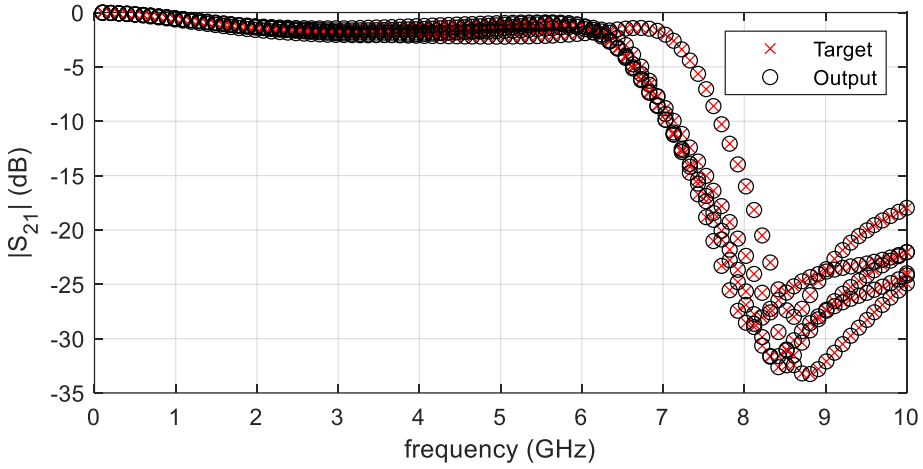

Fig. 3.4 Comparison of COMSOL (o) and Bayesian ANN (x) model responses for the 10 random temperature testing base points.

3.4. Conclusions

In this chapter, a comparison between three artificial neural network learning techniques Bayesian Regularization, Resilient BP, and Levenberg–Marquardt BP was performed. The objective was to model the magnitude response $|S_{21}|$ of a multiphysical second-order low-pass filter implemented in COMSOL and subjected to temperature variations. For training the learning base points were simulated within a region of interest and for performance evaluation, 10 random testing base points were generated. A total of 20 ANN models per learning algorithm were developed.

The best model for each technique was selected based on the minimum values of MSE, MLE and MTE. The results demonstrate that the Bayesian Regularization ANN provided the best generalization performance, showing a very good agreement with COMSOL responses at previously unseen testing points. These findings support the suitability of Bayesian ANN models

for accurately representing the multiphysical behavior of high-frequency structures.

4. Advanced Thermal and EM Characterization of Variable-Dimension Low-Pass Filters Using BNN-LHS Integration in COMSOL Simulations

In the rapidly evolving field of electromagnetic (EM) system design, the quest for precision and efficiency has led to the integration of advanced computational methodologies. Among these, Bayesian Neural Networks (BNN) coupled with Latin Hypercube Sampling (LHS) techniques have emerged as a formidable approach for optimizing RF low-pass filters, marking a significant leap in predictive modeling capabilities [Tazifor Tchantcho -23]. This investigation introduces an innovative thermal optimization framework that leverages BNN enhanced with LHS and temperature variables, setting a new standard for low-pass filter modeling [Zhang-23].

The advent of incorporating temperature as a critical variable alongside dimensional parameters, operational frequency and S-parameter values heralds a multiphysical approach in filter performance analysis [Koigerov-22]. Such an approach is not merely an advancement; it represents a paradigm shift towards simulating real-world operational conditions with unprecedented precision [Haghighi-23]. By meticulously refining mesh design to account for thermal effects, our study bridges the gap between theoretical modeling and practical application, ensuring that simulations mirror the complex interplay of electromagnetic and thermal behaviors with high fidelity [Dávalos-Guzmán-23].

Recent advancements in COMSOL Multiphysics predictive modeling have underscored the importance of high-dimensional data analysis in electronics, emphasizing the sensitivity of electronic filters to variability in operational conditions [Nakilcioğlu-22]. Our research builds upon these foundations, introducing a comprehensive methodological approach that integrates temperature into the parameter sweep, thereby enhancing the simulation's accuracy [Pugalenthi-22]. The enhanced BNN training, incorporating temperature alongside physical dimensions and frequency, represents a significant methodological enhancement, expanding the dataset to capture a broad spectrum of operational scenarios [Zeng-23].

The implications of temperature in EM behavior analysis are profound. The integration of thermal considerations into BNN training not only enriches the model's predictive accuracy but

also opens new avenues for the rapid development and optimization of EM components across diverse environmental conditions [Liu-22]. Our findings, supported by a rigorous validation of the BNN model on unseen data, promise transformative impacts in EM simulation and design, suggesting that data-driven design and simulation enhancement can markedly improve the accuracy and efficiency of predictive modeling [Aliqab-23].

4.1. Advanced Thermal Optimization for Predictive Low-Pass Filter Modeling

4.1.1 Mesh Design Enhancement with Thermal Consideration

Building upon the foundation laid in previous simulations, the mesh architecture has been further refined to incorporate thermal influences, a critical factor in the electromagnetic performance of low-pass filter models. This chapter will discuss the strategic development of an advanced mesh that responds to thermal gradients, ensuring that the simulation captures real-world operational conditions with heightened accuracy.

The mesh architecture in finite element analysis shown in Fig. 4.1,

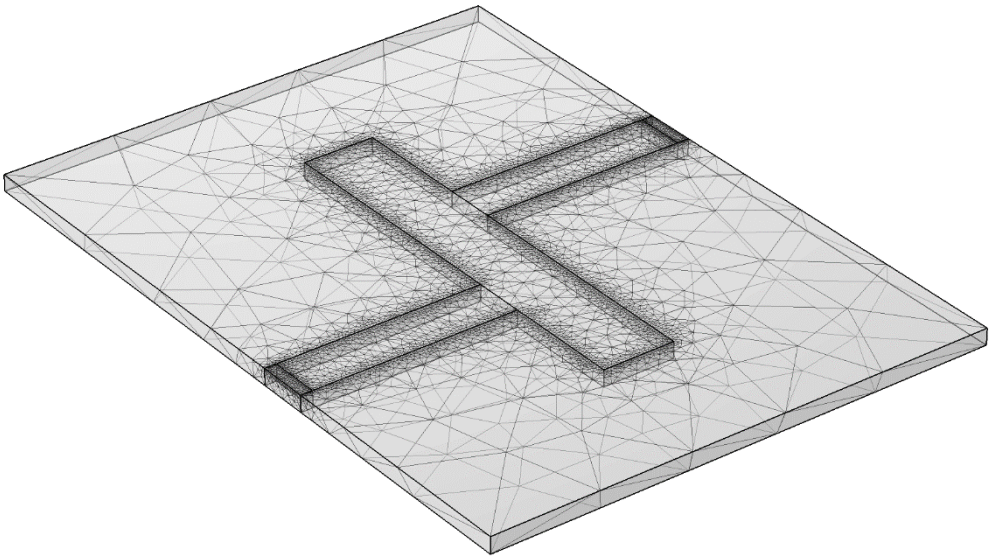

Fig. 4.1 –Finite element mesh of a Low-Pass filter for EM analysis in COMSOL Multiphysics.

Simulation Parameter Description	Value	Identifier
Starting Frequency for Simulation	100 MHz	F_initial
Ending Frequency for Simulation	10 GHz	F_final
Total Frequency Data Points	40 points	N_freq
Smallest Mesh Element Size Overall	0.397 mm	Min_Elem_Size_Global
Largest Mesh Element Size Overall	7.94 mm	Max_Elem_Size_Global
Minimum Mesh Size in Microstrip Line	1.667 mm	Min_Elem_Size_Microstrip
Maximum Mesh Size in Microstrip Line	8.3352 mm	Max_Elem_Size_Microstrip
Smallest Mesh Size in Port Regions	0.2794 mm	Min_Elem_Size_Ports
Largest Mesh Size in Port Regions	2.79 mm	Max_Elem_Size_Ports
Mesh Density in Narrow Regions	High	Mesh_Density_Narrow
Mesh Growth Rate	1.8	Mesh_Growth_Rate

Table 4.1. COMSOL mesh and simulation parameters for Low-Pass filter analysis.

Parameter description	Value	Identifier
Dielectric constant	2.2	ε_r
Substrate layer thickness	0.794 mm	H
Input/Output trace width	2.45 mm	W_p
Input/Output trace length	10 mm	L_p
Gap width between microstrip lines	3.5 mm	W_1
Length of open circuit stubs	5.6 mm	L_1
Distance between feeding stubs	4.2 mm	S_1
Proximity to front edge of substrate	0.5635 mm	x_{gap}
Proximity to side edge of substrate	6.6681 mm	y_{gap}
Height above ground plane	9.528 mm	H_{air}

Table 4.2. Design parameters for COMSOL simulated Low-Pass filter.

is used in this new iteration simulation for thermo-electromagnetic analysis, parameters from Tables 4.1 and 4.2, are meticulously selected to account for both electromagnetic and thermal behaviors. The parameters are defined not only to capture the filter's response over the designated frequency range but also to monitor the effects of temperature fluctuations on the filter's performance shown in Fig. 4.2.

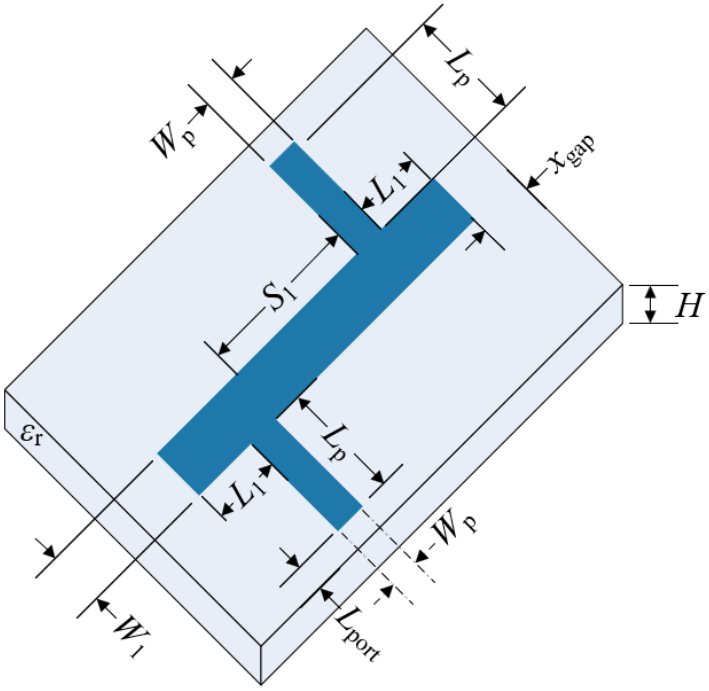

Fig. 4.2 - Detailed schematic of coarse Low-Pass filter dimensions as implemented in COMSOL simulation. Figure taken from [Rayas-Sánchez-12d], to illustrate the physical dimensions of the circuit.

This dual-focused simulation approach is critical for developing filters that are robust across various environmental conditions.

4.1.2 Comprehensive Methodological Approach

The methodology retains its core structure reported in [Dávalos-Guzmán-24], emphasizing the rationale behind the parameter sweep and the LHS technique, with an additional focus on the thermal aspects of filter performance. The rationale for integrating temperature into the parameter sweep is explained, highlighting its importance in the overall simulation accuracy.

4.1.3 Enhanced BNN Training Incorporating Temperature

The training process of the Bayesian Neural Network has been extended to explicitly incorporate temperature as a key input variable, alongside geometric parameters and frequency. This enhancement enables the model to capture the combined thermo-electromagnetic behavior of

the low-pass filter, increasing its accuracy under varying operating conditions. To achieve this, the dataset was expanded to include the parameter vector, $\tau = [W_1, L_1, S_1, T, F, S_{21}]$ where W_1, L_1, S_1 represent physical dimensions, T is temperature, F is frequency, and $|S_{21}|$ is the magnitude of the transmission coefficient response. A total of 50 design variations were generated using LHS across the geometric parameter space. Each design was evaluated at 40 distinct frequency points, resulting in 50 designs × 40 frequencies = 2000 training samples.

This enriched dataset ensures a broad and representative sampling of the design space, including the thermal domain. The inclusion of temperature as an input variable allows the BNN to learn complex multiphysical dependencies, thus improving its ability to generalize to unseen conditions, such as thermal drift or structural deformation. To further enhance realism, the COMSOL simulation configuration was refined to include accurate thermal material properties and boundary conditions. These parameters govern how heat propagates through the structure and interacts with electromagnetic fields, enabling the simulation results to reflect realistic physical behavior.

By integrating this refined dataset and multiphysics aware configuration, the BNN model achieves greater robustness in predicting filter responses across both geometric and thermal variations. This positions the BNN framework as a powerful surrogate modeling approach for thermally aware EM circuit design and optimization.

4.1.4 Neural Complexity and Error Dynamics in Multiphysical Filter Optimization

The progression of BNN sophistication in this study has culminated in an advanced multiphysical framework, discernibly illustrated by Fig. 4.3,

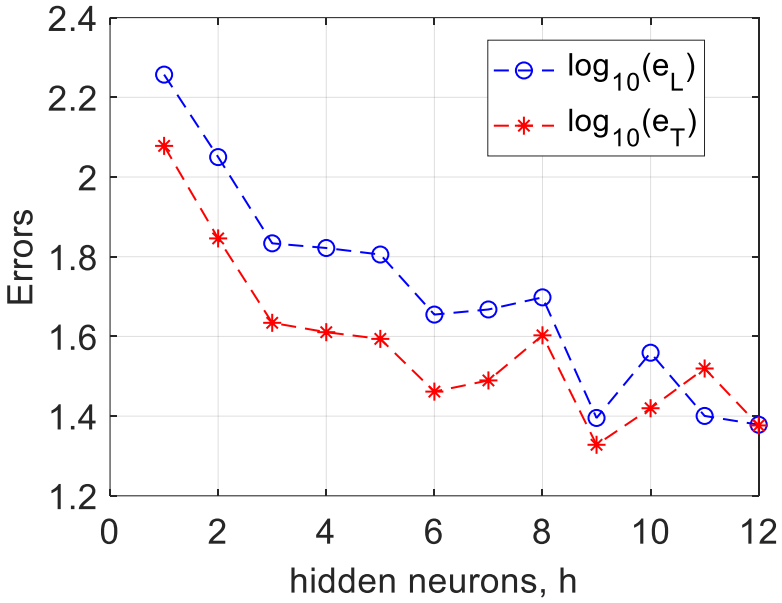

Fig. 4.3 – Plotted errors dynamics with varying hidden neurons in a .1/50 sampled BNN corresponding to the base-10 logarithm of the MSE values for both training $\log_{10}(e_T)$ in red lane, testing datasets $\log_{10}(e_L)$ in the blue lane and corresponding number of hidden neurons h for each ANN training algorithm.

which delineates the learning and testing error patterns as a function of hidden neuron variations in a finely sampled BNN environment. This section dissects the correlation between network complexity and error metrics, highlighting the nuanced impact of temperature integration on predictive precision.

The graphical analysis portrays a clear trend: the learning and testing errors exhibit a decrease as the hidden neuron count rises, up to an inflection point beyond which the benefits plateau, or even regress. This inflection represents an optimal neural complexity, balancing computational load with predictive accuracy.

4.1.5 Implications of Temperature in Modeling

With temperature now a variable in the BNN training, the model navigates a more complex predictive terrain. The analysis indicates a critical intersection where neuron count and thermal factors interplay, suggesting a sweet spot where temperature-induced variabilities are effectively captured without overfitting, as evidenced by the minimal MSE at the .1/50 sampled configuration.

The findings from the .1/50 sampled BNN offer an empirical benchmark for future modeling endeavors. The lowest MSE observed suggests that with careful calibration, a BNN can account for both dimensional and thermal variabilities with high fidelity, setting the stage for a comprehensive approach to filter optimization that is both robust and sensitive to a spectrum of operational influences.

4.2. Enhanced Multiphysical Analysis for Optimizing RF Low-Pass Filters with BNN-LHS Framework

The integration of BNN with LHS has been significantly advanced to include a multiphysical context, notably incorporating temperature as a pivotal variable alongside dimensional variations (W_1, L_1, S_1), operational frequency (F), and $|S_{21}|$ parameter values.

This comprehensive multiphysical analysis of the BNN training results shown in Table 4.3

Variation & Sample Count	*MSE (Accuracy)*	*LE (%)*	*Testing Generalization (%)*	*Network Complexity (Neurons)*
0.1/50	0.4083	17.7516	31.9933	11
0.2/50	0.4699	20.3328	35.2395	13
0.25/50	0.4855	11.6722	33.3739	15
0.15/50	0.4993	13.0466	25.4227	14
0.3/50	1.428	24.6704	35.8113	12

Table 4.3 - BNN's performance sorted from the best to worst testing generalization performance (MSE) across dimensional variations.

Unravelling the intricate interplay between these variables and their collective influence on the predictive accuracy of RF low-pass filter models. Utilizing a dataset of 2000 samples, which merges 50 LHS points with a frequency sweep across 40 points, lays a robust foundation for our investigation.

4.2.1 Experimental Setup and Findings

Our exploration across dimension variations from 0.1% to 0.3% has unveiled nuanced insights into the model's performance under different configurations. The MSE serving as our primary accuracy metric reveals a general trend where an increase in variation correlates with a

rise in MSE, indicating a decrement in model accuracy. A significant spike in MSE at a 0.3% variation marks a notable decrease in accuracy, likely stemming from the model's difficulty in generalizing across extensive data variation.

Further in depth our analysis is provided by MLE and MTE metrics. The highest learning efficiency at the greatest variation suggests that while the model effectively learns from the training data, this does not necessarily translate to improved accuracy or generalization, as evidenced by the elevated MSE. Conversely, the lowest testing generalization, observed at a 0.15% variation, indicates a more harmonious balance between learning and generalization, despite a higher MSE.

Network complexity, indicated by the number of neurons used, shows slight variation across experiments. Intriguingly, the configuration with the highest MSE employed fewer neurons, highlighting that network complexity alone is not the sole determinant of model performance. Rather, the synergy between network complexity and data variation is crucial.

4.2.2 Multiphysical insights

The 0.1/50 configuration, showcasing the lowest MSE of 0.4083, sets a benchmark for the model's highest accuracy at minimal dimensional variation. This outcome is pivotal, establishing a baseline for accuracy against which the impact of additional complexities, such as increased variation or the introduction of temperature, can be measured.

A complex relationship emerges where increased dimension variation initially leads to a slight uptick in predictive errors, as evidenced by MSE, culminating in a significant spike at the highest variation (0.3%). This pattern suggests the model's struggle with accurately predicting the effects of larger dimensional variations, a challenge further exacerbated by the introduction of temperature.

The integration of temperature as a variable introduces a layer of complexity that significantly influences MSE outcomes. This addition is critical in understanding the observed increase in MSE at higher variations, suggesting the model's attempts to integrate temperature effects into EM behavior predictions. Achieving optimal model performance necessitates a delicate balance between dimension variation, learning efficiency, and network complexity. The configuration with a 0.15% variation emerges as potentially optimal, characterized by a relatively lower MSE and superior testing generalization. This finding underscores the importance of

balancing various factors to achieve the best possible MSE accuracy.

4.3. Unseen Data Analysis for Bayesian Neural Network Efficacy

Through this validation and error analysis, we not only affirm the BNN model's predictive accuracy but also illuminate pathways for its continuous improvement. These insights are crucial for refining the model, enhancing its predictive precision, and ensuring its readiness for real-world applications. The findings from this section not only demonstrate the model's current capabilities but also lay the groundwork for future enhancements, promising a new era of efficiency and accuracy in EM analysis. The efficacy of the Bayesian Neural Network (BNN) in predicting unseen data is a crucial determinant of its practical utility in electromagnetic (EM) filter design. A focused analysis, as presented in Fig. 4.4,

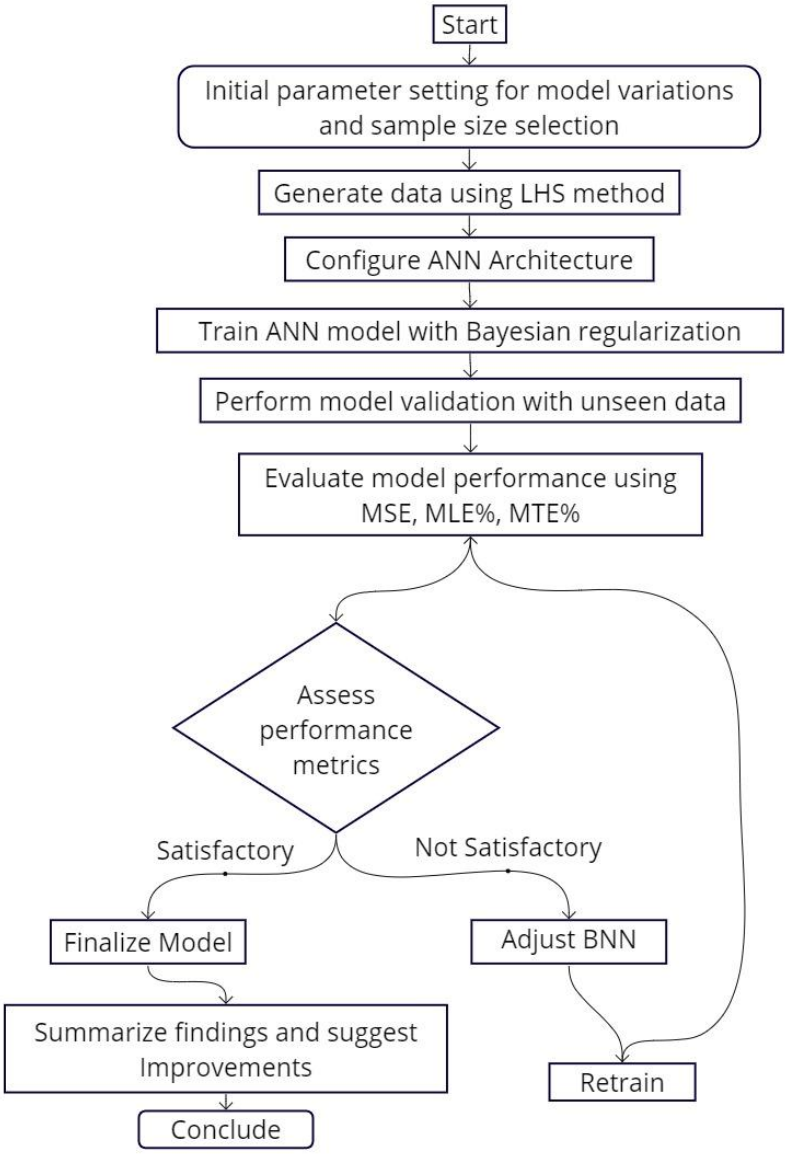

Fig. 4.4 - Optimized training and validation workflow for BNN with dimensional sampling.

scrutinizes the BNN's performance, revealing the model's capability to generalize beyond the training dataset and accurately predict the $|S_{21}|$ parameter in low-pass filters.

4.4. Unseen Data Prediction Validation

To evaluate the generalization capability of the Bayesian Neural Network, a dedicated validation dataset was constructed using a design variation amplitude of 0.1 and 1,000 sampling

points, generated from 25 LHS based input configurations × 40 frequency points.

The scatter plot in Fig. 4.5 illustrates the prediction performance of the trained BNN model on this unseen testing dataset,

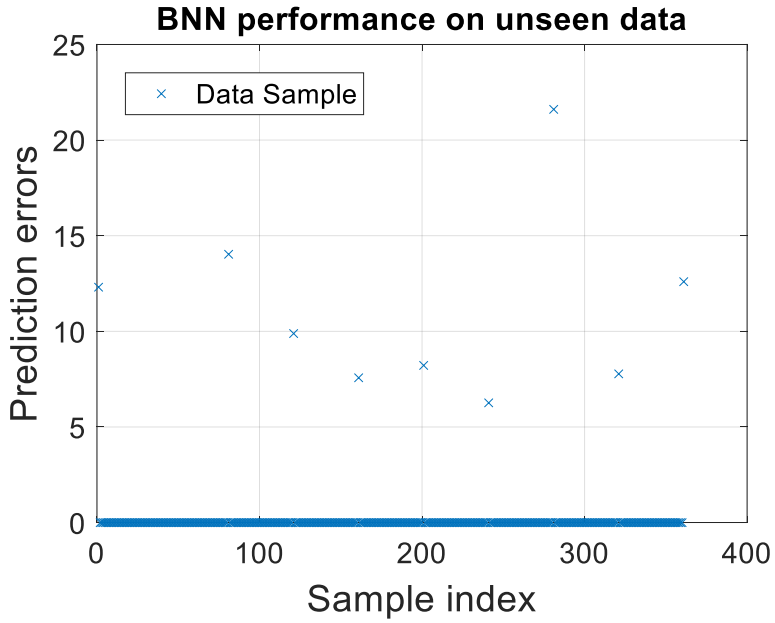

Fig. 4.5 - Scatter plot of predictive validation for BNN on unseen data using $\tau = .1$ and 1000 sampling points.

Each point in Fig. 4.6 represents the comparison between the predicted and actual $|S_{21}|$ values for a given test sample. The proximity of the lines indicates a high level of agreement between the BNN predictions and the COMSOL simulation results, confirming the model's strong generalization to previously unseen data. This predictive validation highlights the BNN's ability to maintain accuracy not only within the training domain but also across perturbed geometrical and thermal conditions, reinforcing its suitability as a surrogate model for multiphysical EM analysis.

The validation of BNN on unseen data is not merely a measure of model performance but also a testament to the model's adaptability and reliability in practical applications. The insights gained from this analysis have profound implications for future EM simulations, where predictive accuracy is paramount. The analysis provides a foundation for continuous model enhancement, with a focus on addressing the outliers and improving the generalization capabilities of the BNN. Future research may delve into advanced machine learning strategies to mitigate prediction errors

further and bolster the model's robustness.

4.5. Results

This new study extended the BNN framework to include temperature variations, enhancing the predictive accuracy for $|S_{21}|$ transmission coefficients within the RF spectrum. The comparative analysis presented in Fig. 4.6,

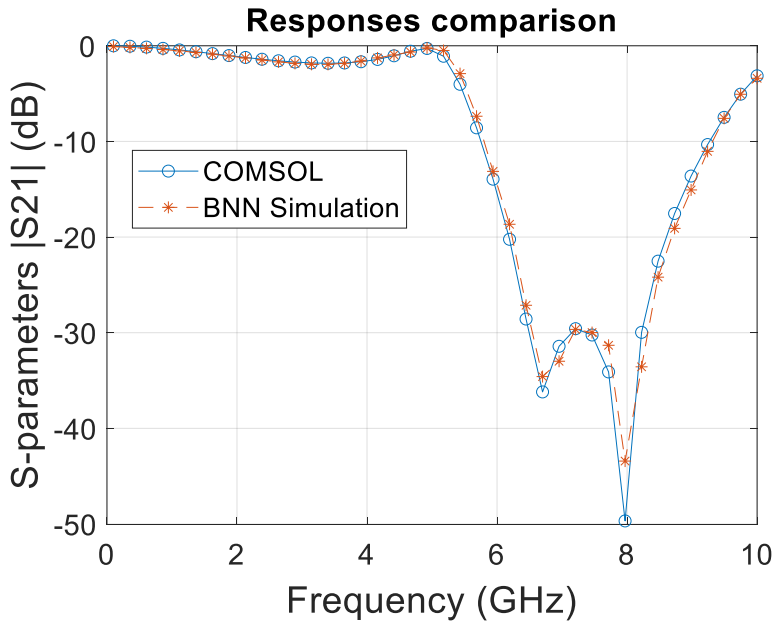

Fig. 4.6 - Comparative analysis of $|S_{21}|$ transmission coefficients from COMSOL and BNN best predictions 0.1/50 from table 4.3 from 0.1-10GHz.

Spanning a frequency range of 0.1-10GHz demonstrates a remarkable alignment between BNN outputs and COMSOL simulations, reinforcing the BNN's ability to internalize and replicate complex EM behaviors.

The graph meticulously compares the $|S_{21}|$ transmission coefficients, a crucial performance metric, obtained from the esteemed COMSOL Multiphysics software against those predicted by the BNN model. The congruence of the curves throughout the frequency sweep, especially at critical resonance frequencies, signifies not only the precision of the BNN but also its potential as a tool for rapid prototyping and iterative design processes. The study underscores the significance of incorporating multiphysical parameters, such as temperature, in the training

dataset to mirror the accuracy of traditional simulation methods while surpassing their efficiency.

Such fidelity in predictive modeling heralds a transformative era in EM simulation, where BNNs can expedite the design cycle without compromising on the accuracy of resonance peak predictions. This leap in simulation technology could redefine the efficiency of EM filter design, with direct implications for industries relying on precise and rapid development cycles.

The slight deviations observed between the BNN predictions and COMSOL results suggest an avenue for further refinement, potentially through enhanced neural network architectures or deeper training sets encompassing broader operational conditions. The validation of the BNN training regimen sets a precedent for the future integration of machine learning within EM analysis, promising significant strides in predictive accuracy and simulation swiftness.

4.6. Conclusions

In this pivotal chapter, we have advanced the frontiers of predictive modeling for low-pass filter design, integrating the precision of BNN with the robustness of LHS and the critical influence of temperature variables. Our multiphysical approach has proven instrumental in capturing the subtleties of EM behavior, offering a significant leap in simulation, accuracy and efficiency. BNN's adeptness in generalizing from a diverse dataset to unseen conditions marks a paradigm shift towards rapid, data-driven filter optimization. The convergence of our predicted results with established COMSOL simulations across a wide frequency range validates the effectiveness of our model. We envision this framework to be a cornerstone in the future of electronic system design, where the integration of machine learning and thermal dynamics will enable swift and precise characterization of complex EM systems, even in fluctuating environmental conditions. Our findings not only consolidate the current understanding of multiphysical interactions in filter performance but also illuminate the path for next-generation simulation methodologies, emphasizing the need for continual refinement and the exploration of novel data-driven techniques for model enhancement.

5. Precision EM profiling with BNN-LHS Synergy for a Varied-Dimension Coarse Low-Pass Filter via COMSOL Simulations

In response to the escalating complexity of EM systems and the concurrent demand for advanced simulation tools, this study explores the intersection of machine learning and computational physics to enhance EM characterization. Specifically, we integrate BNNs with LHS within COMSOL simulations to analyze variable-dimension coarse low-pass filters. This approach not only aims to predict EM behavior modifications induced by physical dimension variability but also seeks to optimize system modeling through artificial neural networks. The integration of BNNs and LHS represents a novel methodology in the field of EM analysis, offering a promising avenue for achieving high accuracy in simulations while maintaining computational efficiency.

The quest for speed and precision in EM characterization has led to a paradigm shift, where the capabilities of traditional computational physics are significantly enhanced by the predictive power of machine learning. This synthesis not only facilitates a deeper understanding of EM behavior under varying physical dimensions but also streamlines the design and optimization process of EM systems [Güneş-17], [Borisut-20]. By leveraging the strengths of both domains, our study aims to address the challenges posed by the increasing complexity of EM systems, providing a robust framework for the accurate and efficient analysis of low-pass filters [Dávalos-Guzmán-23].

Our methodology exhibits a dual advantage: it upholds the granularity of traditional simulations while dramatically reducing computational demands. This attribute is crucial for facilitating swift design iterations and prototype development, principles that are increasingly vital in the fast-paced realm of electronic design and optimization [Li-17], [Krishna-08]. The focal point of our analysis, the $|S_{21}|$ parameter -a pivotal metric of power transmission in filters- serves as a testament to the effectiveness of our approach, with its variability under different geometric changes rigorously assessed to demonstrate the nuanced understanding our model offers [Uluslu-23], [Calik-19].

By applying a detailed parameter sweep, this research uncovers the nuanced influence of minute dimensional adjustments, presenting a rich analysis that is both comprehensive and computationally prudent. The implications of this research are multifaceted, offering empirical

contributions to electronic design optimization and heralding a new era of data-driven diagnostics within complex EM environments [Unger-11], [Wang-23]. Through the integration of BNNs and LHS, we challenge traditional EM characterization methods, establishing a new benchmark for reliability and resilience in electronic component design and manufacturing [Yangfan-20], [Mahouti-19], [Çalik-21].

Anticipating future research trajectories, this paper will delve into advanced data-driven methodologies like Bayesian optimization [MacKay-92], further refining the BNN model's acumen [Mahouti-14]. Such techniques underscore a future where electronic design is not only data-informed but also significantly more efficient, marking a significant step forward in the integration of machine learning with computational physics to address the evolving challenges in EM system design and optimization.

5.1. Optimizing Mesh Design and Simulation Parameters for Enhanced EM Filter Analysis in COMSOL

5.1.1 Mesh Design and Justification

The mesh architecture in finite element analysis shown in Fig. 5.1, is a critical determinant of simulation fidelity.

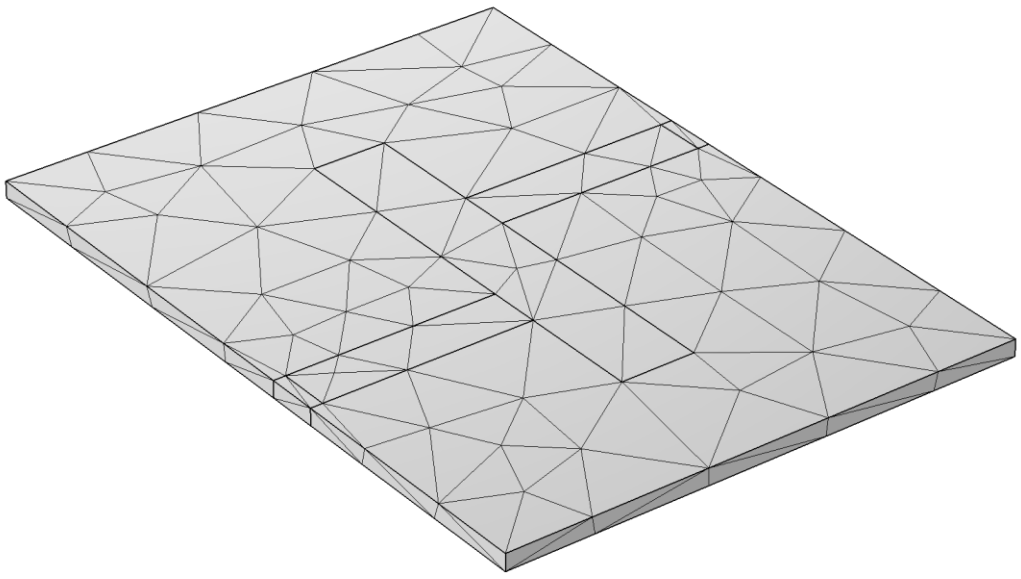

Fig. 5.1 –Finite element mesh of a Low-Pass filter for EM analysis in COMSOL

Multiphysics.

For the COMSOL simulation of our low-pass filter model, the mesh was meticulously designed to optimize the resolution of electromagnetic phenomena. Elements were refined at interfaces where we anticipate significant field gradients, ensuring precise characterization of the filter's response. This strategic densification of mesh elements was particularly employed in areas proximate to the microstrip lines and port regions, where boundary conditions are known to induce complex field interactions. The sensitivity of the simulation outcomes to mesh variation was assessed, ensuring that our model's predictions remain robust across a spectrum of mesh densities. By optimizing mesh design and simulation parameters, we aim to achieve a balance between computational efficiency and the accuracy required for high-fidelity EM analysis. This optimization is crucial for accurately capturing the nuanced effects of physical dimension variability on filter performance.

5.1.2 Simulation parameters

Each simulation parameter was chosen with the dual objectives of capturing the intricate behavior of the low-pass filter and ensuring the practicality of simulation runs. The starting frequency of 100 MHz and ending frequency of 10 GHz encompass the operational bandwidth, with a total of 40 frequency data points providing a comprehensive frequency response profile. Mesh element sizes were determined based on the geometric intricacies of the filter design and the need to resolve narrow regions with high mesh density, ensuring the capture of subtle effects on the filter's performance. The parameters shown in Table 5.1.

underpin the robustness and precision of our simulation outcomes. Through rigorous validation against theoretical expectations and empirical benchmarks, the model's computational integrity is demonstrated, thus bolstering the confidence in our simulation-based predictions.

A structured approach to optimizing the performance of radiofrequency (RF) low-pass filter shown in Fig. 5.2

Simulation Parameter Description	Value	Identifier
Starting Frequency for Simulation	100 MHz	F_initial
Ending Frequency for Simulation	10 GHz	F_final
Total Frequency Data Points	40 points	N_freq
Smallest Mesh Element Size Overall	0.397 mm	Min_Elem_Size_Global
Largest Mesh Element Size Overall	7.94 mm	Max_Elem_Size_Global
Minimum Mesh Size in Microstrip Line	1.667 mm	Min_Elem_Size_Microstrip
Maximum Mesh Size in Microstrip Line	8.3352 mm	Max_Elem_Size_Microstrip
Smallest Mesh Size in Port Regions	0.2794 mm	Min_Elem_Size_Ports
Largest Mesh Size in Port Regions	2.79 mm	Max_Elem_Size_Ports
Mesh Density in Narrow Regions	High	Mesh_Density_Narrow
Mesh Growth Rate	1.8	Mesh_Growth_Rate

Table 5.1. COMSOL mesh and simulation parameters for Low-Pass filter analysis.

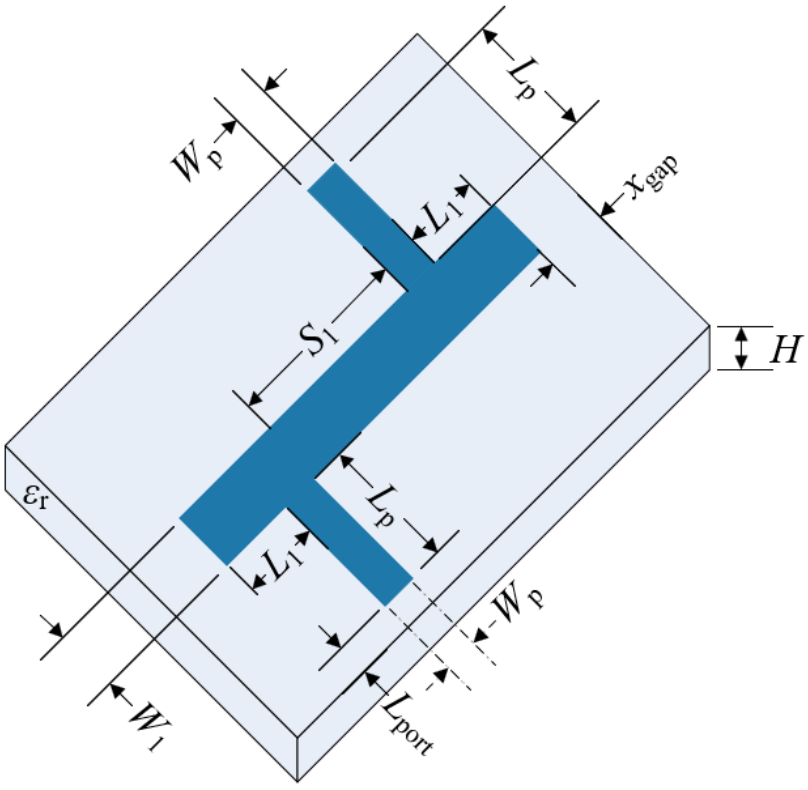

Fig. 5.2 - Detailed schematic of coarse Low-Pass filter dimensions as implemented in COMSOL simulation. Figure taken from [Rayas-Sánchez-12d], to illustrate the physical dimensions of the circuit.

using a BNN trained with LHS data is followed. The meticulous parameter sweep aims to refine the filter design by adjusting physical dimensions width (W_1), length (L_1), and spacing (S_1) to assess their influence on the filter's electromagnetic behavior.

5.1.3 Parameter Sweep and LHS Technique

A targeted sweep varying from 0.1% to 0.3% for the dimensions W_1, L_1, and S_1 was executed to precisely gauge their effects on filter performance at high frequencies. Coupled with the LHS method, this facilitated a nuanced exploration of the design space, ensuring a robust data set that reflects the diverse operational conditions of the filter.

5.1.4 Bayesian Neural Network Training

The BNN was trained using a dataset featuring five key variables: W_1, L_1, and S_1, operational frequency (F), and $|S_{21}|$ parameter values, representing the transmission power through the filter. This comprehensive training set was derived from the integration of LHS and empirical data, providing a strategic balance of dimensional variables and operational frequencies, encapsulated in a dataset of 2000 entries.

5.1.5 Data Set Composition

The dataset's adequacy is demonstrated by its breadth, covering 40 frequency points across 50 distinct sampling regions, thereby ensuring that the BNN model is exposed to a wide spectrum of potential operational scenarios. This variety is critical for the model's ability to generalize and predict accurately across different environmental conditions and design configurations.

5.1.6 Integration of COMSOL design parameters

In conjunction with the BNN training, specific design parameters from COMSOL simulations were systematically incorporated to enhance the model's predictive accuracy. The parameters, detailed in Table 5.2,

Parameter description	Value	Identifier
Dielectric constant	2.2	ε_r
Substrate layer thickness	0.794 mm	H
Input/Output trace width	2.45 mm	w_p
Input/Output trace length	10 mm	L_p
Gap width between microstrip lines	3.5 mm	w_1
Length of open circuit stubs	5.6 mm	L_1
Distance between feeding stubs	4.2 mm	S_1
Proximity to front edge of substrate	0.5635 mm	x_{gap}
Proximity to side edge of substrate	6.6681 mm	y_{gap}
Height above ground plane	9.528 mm	H_{air}

Table 5.2. Design parameters for COMSOL simulated Low-Pass filter.

Including the dielectric constant (ε_r), substrate layer thickness (H), and various dimensions pertinent to the filter's microstrip layout. Each parameter plays a pivotal role in shaping the electromagnetic responses of the filter, and their careful selection is reflective of the filter's operational environment and design requirements. Table 5.2 outlines the design parameters employed in the COMSOL simulations for the low-pass filter, linking each to its identifier and providing a value that aligns with the study's goals.

5.2. Advanced BNN-LHS Integration for RF Low-Pass Filter Optimization and Performance Analysis

The integration of BNN with LHS represents a novel approach to RF low-pass filter optimization, allowing for a more granular exploration of the design space. This methodology not only enhances the precision of our simulations but also significantly reduces the computational resources required, aligning with our goal of streamlining the design process.

The performance metrics of a BNN training for different configurations measured in terms of MSE, MLE, and MTE are shown in Table 5.3,

Variation & Sample Count	MSE (Accuracy)	LE (%)	Testing Generalization (%)	Network Complexity (Neurons)
.15/50	0.2903	11.3117	15.9565	13
.2/50	0.3365	30.4209	36.0903	11
.1/50	0.7454	12.3728	35.9268	10
.25/50	0.8921	23.4974	38.28	10
.3/50	2.6578	24.1204	47.856	13

Table 5.3 - BNN's performance sorted from the best to worst testing generalization performance (MSE) across dimensional variations.

along with the number of neurons used in the network. Fig. 5.3,

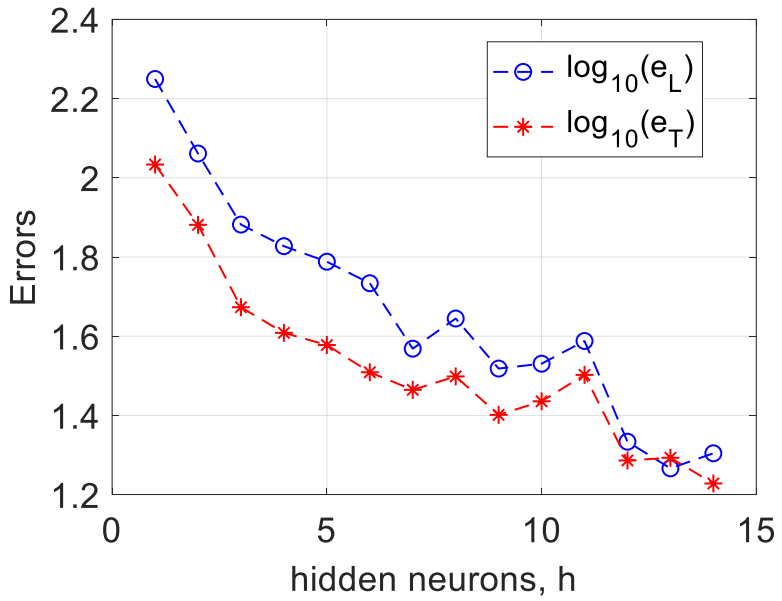

Fig. 5.3 –Plotted errors dynamics with varying hidden neurons in a .15/50 sampled BNN corresponding to the base-10 logarithm of the MSE values for both training $\log_{10}(e_T)$ in red lane, testing datasets $\log_{10}(e_L)$ in the blue lane and corresponding number of hidden neurons h for each ANN training algorithm.

illustrates the logarithmic scale of learning and testing errors denoted by $\log_{10}(e_L)$ and $\log_{10}(e_T)$ respectively as a function of the number of hidden neurons in the network.

The MSE is lowest at 0.2903 for the configuration with a 0.15 percentage variation and 50

samples. This suggests that this setup was the most effective at predicting the target parameter, likely due to an optimal balance between overfitting and underfitting the data. As the percentage variation increases from 0.15 to 0.3, the MSE increases significantly, indicating a decrease in predictive accuracy. This might be due to the model overfitting to noise in the data or not being complex enough to capture the underlying relationship at higher variation levels.

The MLE is relatively low for the 0.15/50 and 0.1/50 configurations, which could imply that the model is learning the training data efficiently without overfitting. A significant spike in MLE for the 0.2/50 configuration indicates that the model might be overfitting the training data or that the increase in parameter variation is introducing complexity that the model cannot learn effectively.

The MTE is reasonably low for the 0.15/50 configuration, suggesting good model generalization to unseen data. Higher MTE values in other configurations, especially 0.25/50 and 0.3/50 highlight a degradation in the model's ability to generalize. This could be due to the model learning specific patterns in the training data that do not apply to the test data.

The number of neurons used does not show a direct correlation with better performance across all metrics. For instance, the 0.15/50 configuration uses 13 neurons and has the best MSE, while the 0.3/50 configuration also uses 13 neurons but has the worst performance metrics. This indicates that simply increasing the number of neurons is not a guarantee of improved performance. It's the combination of the right number of neurons and the appropriate level of input variation that results in the most accurate predictions. The goal in model development should be to aim for the lowest MSE while maintaining a reasonable balance between MLE% and MTE% to avoid overfitting and ensure good generalization to unseen data.

5.3. Model Validation and Error Analysis for Predictive Accuracy Enhancement

The validation and error analysis of our BNN model are pivotal in ensuring its robustness and practical applicability for EM system design and optimization. This comprehensive process, illustrated in Fig. 5.4,

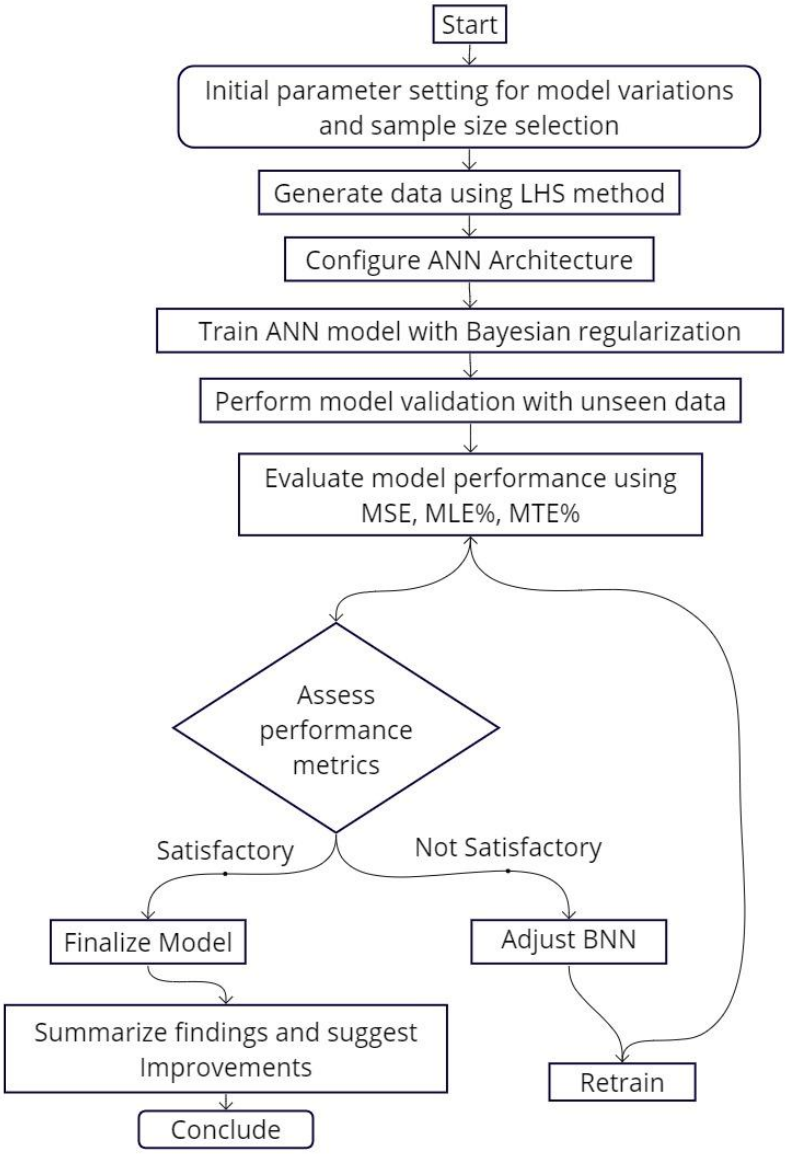

Fig. 5.4 - Optimized training and validation workflow for BNN with dimensional sampling.

is essential for transitioning theoretical models into practical solutions that significantly impact the efficiency and effectiveness of EM characterizations in real-world scenarios.

In validating our BNN model and analyzing prediction errors, we delve deep into the model's performance, identifying opportunities for refinement and enhancement. This meticulous analysis is instrumental in advancing the model's practical applicability, setting the stage for its integration into the design and optimization of EM systems. By examining where and why certain predictions deviate from expected outcomes, as shown in Fig. 5.5,

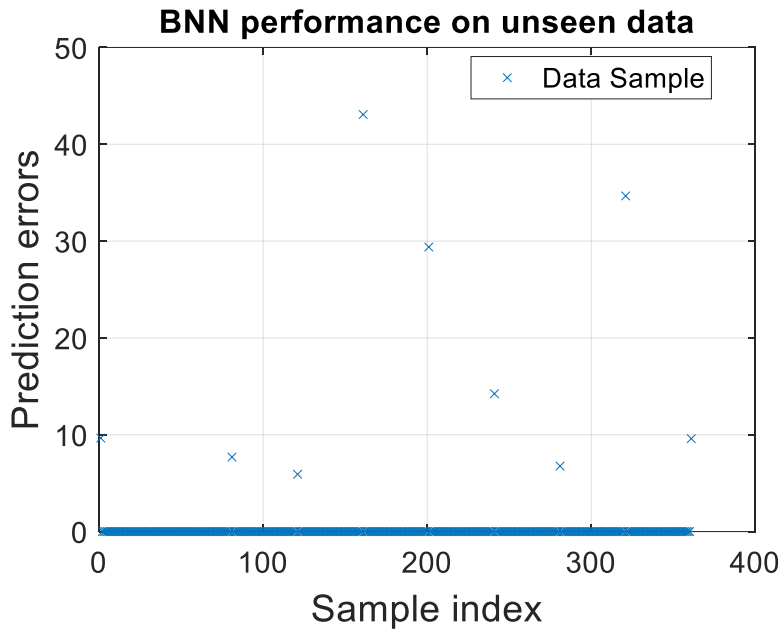

Fig. 5.5 - Scatter plot of predictive validation for BNN on unseen data using $\tau = .15$ and 1000 sampling points

we can pinpoint areas for improvement in the model's architecture, training process, or data preprocessing strategies.

The distribution of prediction errors for unseen data samples reveals a concentration of data points towards the lower end of the prediction error scale, affirming the BNN's efficacy in accurately forecasting most test cases. However, the presence of outliers with significantly higher prediction errors highlights instances where the model's forecasts diverge markedly from the actual values. These outliers are invaluable for identifying the model's limitations and areas necessitating refinement.

Moreover, the consistent performance of the model across various subsets of unseen data underscores its robust generalization capability. It indicates that the BNN has successfully captured the underlying patterns rather than merely memorizing the training data. The aggregation of predictions near the zero-error line for a substantial portion of the data suggests that the model's features and architecture are aptly suited for the task. Nonetheless, regions with elevated errors signal potential overfitting issues, where the model excels with training data but falters in predicting new, unseen data. This discrepancy may stem from an overly complex model or training data that fails to represent the full spectrum of variability in unseen data.

Through this validation and error analysis, we not only affirm the BNN model's predictive

accuracy but also illuminate pathways for its continuous improvement. These insights are crucial for refining the model, enhancing its predictive precision, and ensuring its readiness for real-world applications. The findings from this section not only demonstrate the model's current capabilities but also lay the groundwork for future enhancements, promising a new era of efficiency and accuracy in EM analysis.

5.4. Results

Both the COMSOL and BNN curves shown in Fig. 5.6,

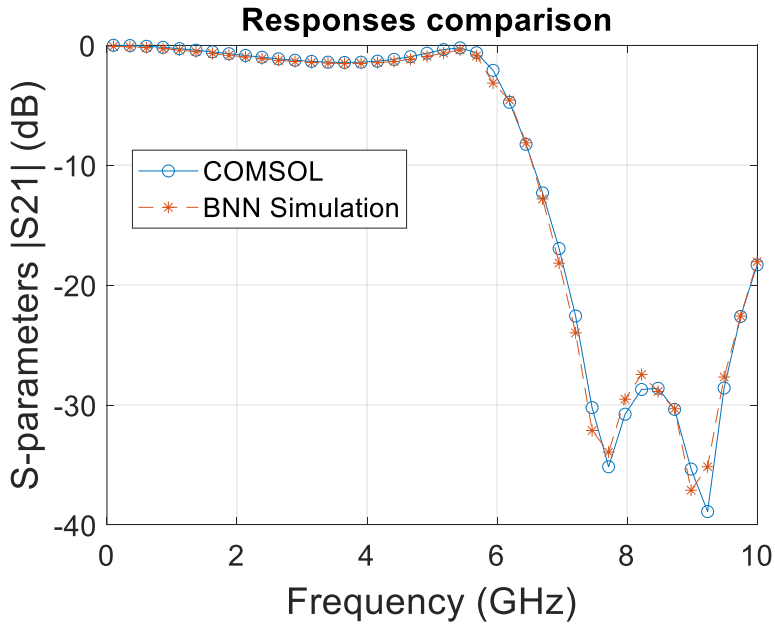

Fig. 5.6 - Comparative analysis of $|S_{21}|$ transmission coefficients from COMSOL and BNN best predictions 0.15/50 from table 5.3 from 0.1-10GHz.

closely follow each other, which indicates a high degree of correlation between the simulated data and the BNN predictions. This suggests that the BNN has effectively learned the underlying physical phenomena governing the system's behavior over the frequency sweep. The BNN has successfully captured the resonance peaks, which are critical in filter design as they represent frequencies at which the filter significantly attenuates the signal. The accuracy in predicting these peaks is essential for the validation of the neural network model in practical applications.

Our findings demonstrate a high degree of correlation between BNN predictions and COMSOL simulations, validating our approach. This correlation not only underscores the effectiveness of our BNN-LHS integration but also suggests potential applications in streamlining the design and optimization of EM components. Comparing these results with our previous methodologies highlights the advantages of our approach in terms of both accuracy and efficiency.

The close matching of the BNN predictions to the COMSOL simulations across the entire frequency range demonstrates the model's fidelity. It is particularly adept at capturing the filter's behavior both in the passband (low attenuation regions) and the stopband (high attenuation regions). The predictive performance of the BNN is exemplified in the regions where the $|S_{21}|$ response is changing rapidly, such as the steep slopes leading into and out of the resonance valleys. BNN's ability to predict these changes is indicative of a well-trained model that understands the frequency-dependent characteristics of the filter.

While the overall match is quite good, any discrepancies, even minor ones, between the BNN predictions and the COMSOL simulations should be noted. These could indicate areas where the model may require further training or where the complexity of the physical system may necessitate a more sophisticated neural network architecture. The graph serves as a validation of the BNN training process, indicating that the chosen architecture, learning rate, and number of epochs are likely well-suited for this type of prediction task.

Importantly, one of the most compelling advantages of using BNNs is the significant reduction in computational time: while a full COMSOL simulation may take approximately 20 minutes per evaluation on a Core i7 machine with 16 GB of RAM, the BNN model can produce a prediction in just 10 to 20 seconds. This efficiency represents a reduction of over 95% in simulation time, enabling rapid design iterations and parameter sweeps. The ability of the BNN to closely predict COMSOL responses thus offers a powerful tool to accelerate the design process by providing fast, accurate evaluations of system performance across a range of frequencies without the need for repeated full-wave simulations.

5.5. Conclusions

This chapter has highlighted the transformative potential of BNNs in the realm of EM system analysis, showcasing a significant leap in the fusion of machine learning techniques with

traditional simulation methodologies. Through the adept integration of BNNs with LHS, we have demonstrated a methodological innovation that not only enhances the precision of EM characterizations but also optimizes the design process with remarkable computational efficiency. This improvement in characterization accuracy is quantitatively demonstrated by the low error metrics achieved across training and unseen testing datasets (MSE, MLE, and MTE), along with the strong correlation observed between the BNN predictions and COMSOL simulations. Additionally, the use of LHS ensured efficient sampling of the design space, which further contributed to the robustness and generalization capability of the model.

Our findings reveal the critical role of nuanced parameter adjustments and sampling strategies in elevating model performance, thereby challenging and extending beyond conventional EM analysis approaches. The successful application of BNNs, facilitated by LHS, has opened new avenues for research, especially in hyperparameter optimization and the development of increasingly complex EM components.

This advancement underscores our contribution to both the theoretical framework and practical applications in EM system characterization, with significant implications for the design and manufacturing of electronic components. As we look forward, the potential for further exploration and application of these data-driven methodologies promises to revolutionize the design and optimization of EM systems, paving the way for innovations in electronic systems that are integral to technological progress.

General Conclusions

This doctoral dissertation presents a comprehensive study of advanced modeling and optimization techniques for high-frequency (HF) structures, integrating surrogate modeling, multiphysical considerations, and machine learning approaches. The key findings and methodologies are summarized as follows:

In chapter 1, a method for performing COMSOL Multiphysics simulations of a microstrip low-pass filter driven by MATLAB was introduced. Different meshing schemes for the microstrip were implemented, and simulations were conducted across three temperature ranges. The results demonstrated the significant impact of temperature variations, including the deformation of the air box caused by the expansion and contraction of the inner air, underscoring the importance of considering thermal effects in HF structure simulations.

Chapter 2 detailed the development of electromagnetics-based surrogate models for a low-pass microstrip filter in the frequency domain, accounting for physical dimension variations. Various surrogate modeling techniques, including generalized regression neural networks (GRNN), Kriging, and support vector machines (SVM), were compared. The results indicated that Kriging provided the best performance, with a reasonable match between the fine model responses and the surrogate models developed. This chapter highlighted the importance of selecting appropriate modeling techniques and training regions to achieve high accuracy in surrogate models.

In chapter 3, a comparative analysis of three artificial neural network (ANN) learning techniques Bayesian regularization, Resilient BP, and Levenberg-Marquardt BP was conducted to model the response $|S_{21}|$ of a multiphysical second-order low-pass filter implemented in COMSOL, subject to temperature variations. Bayesian ANN exhibited the best performance, demonstrating a very good match between the COMSOL and Bayesian ANN model responses at testing points. This finding confirmed the suitability of Bayesian ANN for representing the multiphysical response of HF structures, thereby facilitating more accurate and efficient modeling.

In chapter 4 an advanced thermal optimization framework for predictive low-pass filter modeling was proposed, integrating Bayesian Neural Networks (BNN) with Latin Hypercube Sampling (LHS) and temperature variables. This multiphysical approach significantly improved

simulation accuracy and efficiency, capturing the subtleties of EM behavior under varying thermal conditions. The successful generalization of BNNs from diverse datasets to unseen conditions, validated the effectiveness of this approach, positioning it as a cornerstone for future electronic system design that integrates machine learning and thermal dynamics.

In chapter 5, a transformative potential of BNNs in electromagnetic (EM) system analysis was showcased, highlighting the integration of BNNs with LHS to enhance the precision of EM characterizations and optimize the design process. This chapter emphasized the critical role of parameter adjustments and sampling strategies in improving model performance, challenging traditional EM analysis methods. The success of BNNs facilitated by LHS opened new avenues for research, particularly in hyperparameter optimization and the development of complex EM components. This advancement underscores significant contributions to both theoretical frameworks and practical applications in EM system characterization, with implications for the design and manufacturing of electronic components.

This doctoral dissertation offers several promising avenues for future research. One potential direction is to explore the integration of more advanced machine learning techniques, such as deep learning models, to further enhance the accuracy and efficiency of surrogate models. Additionally, the application of these techniques to more complex and diverse HF structures, including those used in emerging technologies like 5G and IoT devices, would be valuable.

Expanding multiphysical simulations to include more comprehensive environmental factors, such as humidity and mechanical vibrations, will also be crucial to study the capability of the proposed techniques in accurately representing EM responses under various physical conditions.

Furthermore, the methodologies proposed are not intrinsically limited to HF structures or the frequency domain and can be applied to other computationally expensive design problems, such as thermal management systems and advanced material design.

Overall, this dissertation demonstrates that advanced surrogate modeling techniques, particularly those exploiting Bayesian Neural Networks and other machine learning approaches, provide a robust and efficient framework for modeling and optimizing high-frequency structures. These methodologies offer significant advantages in terms of computational efficiency and accuracy compared to traditional approaches, paving the way for future innovations in the design and optimization of electronic systems.

Conclusiones Generales

Esta tesis doctoral presenta un estudio exhaustivo de técnicas avanzadas de modelado y optimización para estructuras de alta frecuencia (HF), integrando modelos sustitutos, consideraciones multifísicas y enfoques de aprendizaje automático. Los hallazgos clave y las metodologías se resumen de la siguiente manera:

En el capítulo 1 se introdujo un método para realizar simulaciones en COMSOL Multiphysics de un filtro de paso bajo microstrip impulsado por MATLAB. Se implementaron diferentes esquemas de mallado para el microstrip y se realizaron simulaciones en tres rangos de temperatura. Los resultados demostraron el impacto significativo de las variaciones de temperatura, incluida la deformación de la caja de aire causada por la expansión y contracción del aire interior, subrayando la importancia de considerar los efectos térmicos en las simulaciones de estructuras HF.

En el capítulo 2 se detalló el desarrollo de modelos sustitutos basados en electromagnetismo para un filtro de paso bajo microstrip en el dominio de frecuencia, teniendo en cuenta las variaciones de dimensión física. Se compararon varias técnicas de modelado sustituto, incluidas las redes neuronales de regresión generalizada (GRNN), Kriging y las máquinas de vectores de soporte (SVM). Los resultados indicaron que Kriging proporcionó el mejor rendimiento, con una correspondencia razonable entre las respuestas del modelo fino y los modelos sustitutos desarrollados. Este capítulo destacó la importancia de seleccionar técnicas de modelado y regiones de entrenamiento apropiadas para lograr una alta precisión en los modelos sustitutos.

En el capítulo 3 se realizó un análisis comparativo de tres técnicas de aprendizaje de redes neuronales artificiales (ANN): regularización bayesiana, Resilient BP y Levenberg-Marquardt BP, para modelar la respuesta $|S_{21}|$ de un filtro de paso bajo de segundo orden multifísico implementado en COMSOL, sujeto a variaciones de temperatura. La ANN bayesiana exhibió el mejor rendimiento, demostrando una muy buena correspondencia entre las respuestas del modelo COMSOL y el modelo ANN bayesiano en los puntos de prueba. Este hallazgo confirmó la idoneidad de la ANN bayesiana para representar la respuesta multifísica de estructuras HF, facilitando así un modelado más preciso y eficiente.

En el capítulo 4, se propuso un marco avanzado de optimización térmica para el modelado

predictivo de filtros de paso bajo, integrando redes neuronales bayesianas (BNN) con muestreo de hipercubo latino (LHS) y variables de temperatura. Este enfoque multifísico mejoró significativamente la precisión y eficiencia de la simulación, capturando las sutilezas del comportamiento electromagnético (EM) bajo condiciones térmicas variables. La generalización exitosa de las BNN a partir de conjuntos de datos diversos a condiciones no vistas validó la efectividad de este enfoque, posicionándolo como una piedra angular para el diseño futuro de sistemas electrónicos que integren aprendizaje automático y dinámica térmica.

En el capítulo 5 se destacó el potencial transformador de las BNN en el análisis de sistemas electromagnéticos (EM), subrayando la integración de las BNN con LHS para mejorar la precisión de las caracterizaciones EM y optimizar el proceso de diseño. Este capítulo enfatizó el papel crítico de los ajustes de parámetros y las estrategias de muestreo en la mejora del rendimiento del modelo, desafiando los métodos tradicionales de análisis EM. El éxito de las BNN facilitado por LHS abrió nuevas vías de investigación, particularmente en la optimización de hiper-parámetros y el desarrollo de componentes EM complejos. Este avance subraya contribuciones significativas tanto a los marcos teóricos como a las aplicaciones prácticas en la caracterización de sistemas EM, con implicaciones para el diseño y la fabricación de componentes electrónicos.

Esta tesis doctoral ofrece varios caminos prometedores para futuras investigaciones. Una posible dirección es explorar la integración de técnicas de aprendizaje automático más avanzadas, como modelos de aprendizaje profundo, para mejorar aún más la precisión y eficiencia de los modelos sustitutos. Además, sería valioso aplicar estas técnicas a estructuras HF más complejas y diversas, incluidas las utilizadas en tecnologías emergentes como 5G y dispositivos IoT.

Expandir las simulaciones multifísicas para incluir factores ambientales más completos, como la humedad y las vibraciones mecánicas, también será crucial para estudiar la capacidad de las técnicas propuestas en representar con precisión las respuestas EM bajo diversas condiciones físicas.

Además, las metodologías propuestas no están intrínsecamente limitadas a estructuras HF o al dominio de frecuencia y pueden aplicarse a otros problemas de diseño computacionalmente costosos, como los sistemas de gestión térmica y el diseño de materiales avanzados.

En resumen, esta tesis demuestra que las técnicas avanzadas de modelado sustituto, particularmente aquellas que explotan redes neuronales bayesianas y otros enfoques de aprendizaje automático, proporcionan un marco robusto y eficiente para modelar y optimizar estructuras de

alta frecuencia. Estas metodologías ofrecen ventajas significativas en términos de eficiencia computacional y precisión en comparación con los enfoques tradicionales, allanando el camino para futuras innovaciones en el diseño y la optimización de sistemas electrónicos.

Appendix

Table I - Summary of Matlab ANN training algorithms and default hyperparameters used in this Thesis

Function	Algorithm	Description	Default Hyperparameters
trainlm	Levenberg–Marquardt (BP)	Fast, second-order optimization algorithm that blends gradient descent and Gauss-Newton methods. Recommended for small to medium networks.	- epochs = 1000 - goal = 0 - max_fail = 6 - min_grad = 1e-7 - mu = 0.001 - mu_dec = 0.1 - mu_inc = 10 - mu_max = 1e10 - show = 25 - showWindow = true - time = inf
trainrp	Resilient Backpropagation	Adaptive learning rate method is designed to overcome the drawbacks of pure gradient descent. Suitable for medium-sized problems.	- epochs = 1000 - goal = 0 - max_fail = 6 - delta0 = 0.07 (initial update value) - delta_inc = 1.2 - delta_dec = 0.5 - delta_max = 50 - delta_min = 1e-6 - show = 25 - showWindow = true - time = inf
trainbr	Bayesian Regularization	Modifies the performance function by adding a regularization term. Help avoid overfitting, especially for noisy data.	- epochs = 1000 - goal = 0 - max_fail = 6 - min_grad = 1e-7 - mu = 0.001 - mu_dec = 0.1 - mu_inc = 10 - mu_max = 1e10 - show = 25 - showWindow = true - time = inf - Also applies an automatic adjustment of regularization weights

Table I - Summary of Matlab ANN training algorithms and default hyperparameters used in this Thesis

A. List of internal research reports

1) J. Dávalos-Guzmán, Z. Brito-Brito, and J. E. Rayas-Sánchez, "A brief state of the art on reconfigurable high frequency filters," Internal Report *PhDEngScITESO-18-37-R (CAECAS-18-13-R)*, ITESO, Tlaquepaque, Mexico, Dec. 2018.

2) J. Dávalos-Guzmán, Z. Brito-Brito, and J. E. Rayas-Ernesto "EM simulation of a microstrip low-pass microstrip filter using ADS," Internal Report *PhDEngScITESO-18-60-R*, ITESO, Tlaquepaque, Mexico, Dec. 2018.

3) J. Dávalos-Guzmán, Z. Brito-Brito, and J. E. Rayas-Ernesto "Electromagnetic surrogate modeling of a microstrip low-pass filter," Internal Report *PhDEngScITESO-19-39-R (CAECAS-19-18-R)*, ITESO, Tlaquepaque, Mexico, Dec. 2019.

4) J. Dávalos-Guzmán, Z. Brito-Brito, J. E. Rayas-Sánchez, and J. L. Chávez-Hurtado, "Multiphysics simulation of a microstrip low-pass filter in COMSOL using a Matlab driver," Internal Report *PhDEngScITESO-19-46-R*, ITESO, Tlaquepaque, Mexico, Mar. 2019.

5) J. Dávalos-Guzmán, Z. Brito-Brito, J. E. Rayas-Sánchez, and J. L. Chávez-Hurtado, "Kriging-based surrogate optimization of a microstrip low-pass filter in the frequency domain," Internal Report *PhDEngScITESO-20-22-R (CAECAS-20-10-R)*, ITESO, Tlaquepaque, Mexico, Dec. 2020.

6) J. Dávalos-Guzmán, Z. Brito-Brito, and J. L. Chávez-Hurtado, "Neural network modeling of a synthetic bi-physical second order low-pass filter," Internal Report *PhDEngScITESO-22-09-R*, ITESO, Tlaquepaque, Mexico, Aug. 2022.

7) J. Dávalos-Guzmán, Z. Brito-Brito, and J. L. Chávez-Hurtado, "Neural network modeling of a temperature dependent synthetic second order low-pass filter," Internal Report *PhDEngScITESO-23-04-R*, Tlaquepaque, Mexico, Aug. 2023.

8) J. Dávalos-Guzmán, J. Gómez-López, J. L. Chávez-Hurtado, and Z. Brito-Brito, "A Python-driven approach for advanced design system integration enhancing high-frecuency circuit simulation," Internal Report *PhDEngScITESO-23-08-R*, Tlaquepaque, Mexico, Nov. 2023.

9) J. Dávalos-Guzmán, Z. Brito-Brito, and J. L. Chávez-Hurtado, “Neural network learning techniques comparison for a multiphysics second order low-pass filter,” Internal Report *PhDEngScITESO-23-09-R*, Tlaquepaque, Mexico, Nov. 2023.

10) J. Dávalos-Guzmán, Z. Brito-Brito, J. L. Chávez-Hurtado, and K. Ortstein, “Space sampling techniques comparison for a synthetic low-pass filter bayesian neural network,” Internal Report *PhDEngScITESO-23-14-R*, ITESO, Tlaquepaque, Mexico, Dec. 2023.

11) J. Dávalos-Guzmán, J. L. Chávez-Hurtado, and Z. Brito-Brito, “A bayesian neural network approach with latin hypercube sampling for electromagnetic characterization of synthetical LC circuits,” Internal Report *PhDEngScITESO-23-15-R*, ITESO, Tlaquepaque, Mexico, Dec. 2023.

12) J. Dávalos-Guzmán, J. L. Chávez-Hurtado, and Z. Brito-Brito, “A bayesian neural network approach with latin hypercube sampling for thermo-electromagnetic characterization of synthetical LC circuits,” Internal Report *PhDEngScITESO-24-05-R*, ITESO, Tlaquepaque, Mexico, Feb. 2024.

13) J. Dávalos-Guzmán, J. L. Chávez-Hurtado, and Z. Brito-Brito, “Advanced thermal and EM characterization of variable-dimension low-pass filters using BNN-LHS integration in COMSOL simulations,” Internal Report *PhDEngScITESO-24-06-R*, ITESO, Tlaquepaque, Mexico, Feb. 2024.

14) J. Dávalos-Guzmán, José L. Chávez-Hurtado and, Zabdiel Brito-Brito, “Precision EM Profiling With BNN-LHS Synergy for a Varied-Dimension Coarse Low-Pass Filter Via COMSOL Simulations,” Internal Report *PhDEngScITESO*, ITESO, Tlaquepaque, Mexico, Feb. 2024.

B. List of publications

B.1. Conference papers

1) J. Dávalos-Guzmán, J. L. Chavez-Hurtado, Z. Brito-Brito and K. Ortstein, "Space Sampling Techniques Comparison for a Synthetic Low-Pass Filter Bayesian Neural Network," *2023*

Table I - Summary of Matlab ANN training algorithms and default hyperparameters used in this Thesis

IEEE MTT-S Latin America Microwave Conference (LAMC), San José, Costa Rica, 2023, pp. 109-112, doi: 10.1109/LAMC59011.2023.10375546.

2) J. Dávalos-Guzmán, J. L. Chavez-Hurtado and Z. Brito-Brito, "Neural Network Learning Techniques Comparison for a Multiphysics Second Order Low-Pass Filter," *2023 IEEE MTT-S Latin America Microwave Conference (LAMC)*, San José, Costa Rica, 2023, pp. 102-104, doi: 10.1109/LAMC59011.2023.10375591.

B.2. Journal papers

1) Davalos-Guzman, J., Chavez-Hurtado, J.L., Brito-Brito, Z, Integrative BNN-LHS Surrogate Modeling and Thermo-Mechanical-EM Analysis for Enhanced Characterization of High-Frequency Low-Pass Filters in COMSOL, *Micromachines* **2024**, *15*, 647, doi: 10.3390/mi15050647.

2) Davalos-Guzman, J., Chavez-Hurtado, J.L., Brito-Brito, Z. Accelerating High-Frequency Circuit Optimization Using Machine Learning-Generated Inverse Maps for Enhanced Space Mapping, *Electronics 2025*, 14, 3097, doi: 10.3390/electronics14153097.

Bibliography

[Estrada-Arámbula-11] E. Estrada-Arámbula and J. E. Rayas-Sánchez, "Effects of discontinuities in the reference plane on the performance of microstrip", Internal Report *CAECAS-11-07-R*, ITESO, Tlaquepaque, Mexico, Nov. 2011.

[Vargas-Chávez-11] N. Vargas-Chávez, J. E. Rayas-Sánchez and C. A. López, "Cómo manejar COMSOL Multiphysics 4.1 desde Matlab a través de la línea de comandos", Internal Report *CAECAS-11-09-R*, ITESO, Tlaquepaque, Mexico, Nov. 2011.

[Rayas-Sánchez-12a] J. E. Rayas-Sánchez and Z. Brito-Brito, "Selecting suitable optimization methods for direct optimization of low fidelity model in COMSOL", Internal Report *CAECAS-12-16-R*, ITESO, Tlaquepaque, Mexico, Aug. 2012.

[Jian-Ming Jin-14] Jin, Jian-Ming. *The Finite Element Method in Electromagnetics*. 3rd ed. Wiley, 2014.

[Rayas-Sánchez-12b] J. E. Rayas-Sánchez, J. C. Cervantes-González, Carlos A. López, Z. Brito-Brito and J. Aguilar-Torrentera, "Developing Coarse and fine EM COMSOL models of microstrip low-pass filter for space mapping optimization", Internal Report *CAECAS-12-19-R*, ITESO, Tlaquepaque, Mexico, Sep. 2012.

[Gutiérrez-Ayala-09] V. Gutiérrez-Ayala and J. E. Rayas-Sánchez, "Comparison between three layer perceptrons and two layer perceptrons with optimized nonlinearity for neural space mapping", Internal Report *CAECAS-09-09-R*, ITESO, Tlaquepaque, Mexico, Nov. 2009.

[Rayas-Sánchez-12c] J. E. Rayas-Sánchez and Z. Brito-Brito, "Broyden-based inputs space mapping optimization of microstrip low-pass filter implemented in COMSOL", Internal Report *CAECAS-12-21-R*, ITESO, Tlaquepaque, Mexico, Oct. 2012.

[Dávalos-Guzmán-19a] J. Dávalos-Guzmán, Z. Brito-Brito, J. E. Rayas-Sánchez, and J. L. Chávez-Hurtado, "Multiphysics simulation of a microstrip low-pass filter in COMSOL using a Matlab driver," Internal Report PhDEngScITESO-19-46-R, ITESO, Tlaquepaque, Mexico, Mar. 2019.

[Chávez-Hurtado-16a] J. L. Chávez-Hurtado, Z. Brito-Brito, and J. E. Rayas-Sánchez, "Multiphysics modeling of microwave structures in frequency domain using PSM," Internal Report *PhDEngScITESO-16-21-R (CAECAS-16-12-R)*, ITESO, Tlaquepaque, Mexico, Dec. 2016.

[Song-20] Y. Song, Y. Wen, D. Zhang, and J. Zhang, "Fast prediction model of coupling coefficient between pantograph arcing and GSM-R antenna," *IEEE Transactions on Vehicular Technology*, vol. 69, no. 10, pp. 11612-11618, Aug. 2020.

[Xia-14] B. Xia, Z. Ren, and C. Koh, "Selecting proper kriging surrogate model for optimal design of electromagnetic problem," in *9th IET International Conference on Computation in Electromagnetics (CEM 2014)*, London, UK, Apr. 2014.

[Khandelwal-15] S. Khandelwal, L. Garg, and D. Boolchandani, "Reliability-aware support vector machine-based high-level surrogate model for analog circuits," *IEEE Transactions on Device and Materials Reliability*, vol. 15, no. 3, pp. 461-463, Sep. 2015.

[Chávez-Hurtado-15b] J. L. Chávez-Hurtado and J. E. Rayas-Sánchez, "General formulation for polynomial-based surrogate modeling of microwave structures in frequency domain using the multinomial theorem," Internal Report *PhDEngScITESO-15-12-R (CAECAS-15-14-R)*, ITESO, Tlaquepaque, Mexico, Nov. 2015.

[Chávez-Hurtado-16c] J. L. Chávez-Hurtado, J. E. Rayas-Sánchez, and Z. Brito-Brito, "Multiphysics polynomial-based surrogate modeling of microwave structures in frequency domain," in *IEEE MTT-S Latin America Microwave Conf. (LAMC-2016)*, Puerto Vallarta, Mexico, Dec. 2016.

[Rayas-Sánchez-12d] J. E. Rayas-Sánchez, J. C. Cervantes-González, C. A. López, Z. Brito-Brito and J. Aguilar-Torrentera, "Developing coarse and fine EM COMSOL models of a microstrip low-pass filter for space mapping optimization", Internal Report *CAECAS-12-19-R*, ITESO, Tlaquepaque, Mexico, Sep. 2012.

[Rayas-Sánchez-12e] J. E. Rayas-Sánchez and Z. Brito-Brito, "Broyden-based input space mapping optimization of a microstrip low-pass filter implemented in COMSOL," Internal Report *CAECAS-12-21-R*, ITESO, Tlaquepaque, Mexico, Oct. 2012.

[Chávez-Hurtado-16d] J. L. Chávez-Hurtado, Z. Brito-Brito, and J. E. Rayas-Sánchez, "Multiphysics modeling of microwave structures in frequency domain using PSM," Internal Report *PhDEngScITESO-16-21-R (CAECAS-16-12-R)*, ITESO, Tlaquepaque, Mexico, Dec. 2016.

[More-77] J. J. More, "The Levenberg-Marquardt algorithm: Implementation and theory," in Numerical Analysis, *Lecture Notes in Mathematics*, vol. 630, pp. 105-116, 1977.

[Rumelhart-86] D. E. Rumelhart, G. E. Hinton, and R. J. Williams, "Learning representations by backpropagating errors," *Nature*, vol. 323, no. 6088, pp. 533-536, 1986.

[Waremstein-19] A. Waremstein, N. Balal and Y. Pinhasi, "Reducing Elements in Linear Antenna Array Using Levenberg-Marquardt Algorithm," *2019 13th European Conference on Antennas and Propagation (EuCAP)*, Krakow, Poland, 2019.

[Zhang-20] Huan Huan Zhang, Pan Pan Wang, Shuai Zhang, Long Li, Ping Li, Wei E.I. Sha, and Li Jun Jiang, "Electromagnetic-Circuital-Thermal Multiphysics Simulation Method: A Review (Invited)," *Progress In Electromagnetics Research*, vol. 169, pp. 87-101, Dec. 2020.

[Zhang-19] Huan Huan Zhang, Ying Liu, Wei E.I. Sha, Dazhi Ding, and Zhenhong Fan, "Electromagnetic-Circuital-Thermal Co-Simulation for Integrated Circuits and Microwave Applications," *2019 International Symposium on Antennas and Propagation (ISAP 2019)*, Xi' an, China, Oct. 2019.

[Levenberg-44] M. Levenberg, "A method for the solution of certain non-linear problems in least squares," *Quarterly of Applied Mathematics*, vol. 2, no. 2, pp. 164-168, 1944.

[Marquardt-63] D. W. Marquardt, "An algorithm for least-squares estimation of nonlinear parameters," *Journal of the Society for Industrial and Applied Mathematics*, vol. 11, no. 2, pp. 431-441, 1963.

[Prasad-13] N. Prasad, R. Singh and S. P. Lal, "Comparison of Back Propagation and Resilient Propagation Algorithm for Spam Classification," *2013 Fifth International Conference on Computational Intelligence, Modelling and Simulation*, Seoul, Korea (South), 2013.

[Khan-20] I. Khan et al., "Design of Neural Network With Levenberg-Marquardt and Bayesian Regularization Backpropagation for Solving Pantograph Delay Differential Equations," in *IEEE Access*, vol. 8, pp. 137918-137933, 2020.

[Jafari-10] A. Jafari, S. Sadri and M. Zekri, "Design optimization of analog integrated circuits by using artificial neural networks," *2010 International Conference of Soft Computing and Pattern Recognition*, Cergy-Pontoise, France, 2010.

[Dávalos-Guzmán-19b] J. Dávalos-Guzmán, Z. Brito-Brito, J. E. Rayas-Sánchez, and J. L. Chávez-Hurtado, "Electromagnetic surrogate modeling of a microstrip low-pass filter," Internal Report *PhDEngScITESO-19-39-R (CAECAS-19-18-R)*, ITESO, Tlaquepaque, Mexico, Dec. 2019.

[Zhang-20] G. P. Zhang, "Neural networks for classification: a survey," in *IEEE Transactions on Systems, Man, and Cybernetics, Part C (Applications and Reviews)*, vol. 30, no. 4, pp. 451-462, Nov. 2000.

[Cybenko-89] G. Cybenko, "Approximation by superpositions of a sigmoidal function," *Mathematics of Control, Signals, and Systems*, vol. 2, no. 4, pp. 303-314, Dec. 1989.

[Hornik-89] K. Hornik, M. Stinchcombe, and H. White, "Multilayer feedforward networks are universal approximators," *Neural Networks*, vol. 2, no. 5, pp. 359-366, 1989.

[Tazifor Tchantcho-23] Tazifor Tchantcho, M.; Zimmermann, E.; Huisman, J.A.; Dick, M.; Mester, A.; van Waasen, S., "Low-Pass Filters for a Temperature Drift Correction Method for Electromagnetic Induction Systems" *Sensors,* vol. 23, no. 17, pp. 7322, Aug. 2023.

[Zhang-23] Zhang, Runlin, Nuo Xu, Kai Zhang, Lei Wang, and Gui Lu, "A Parametric Physics-Informed Deep Learning Method for Probabilistic Design of Thermal Protection Systems", *Energies*, vol. 23, no. 16, pp. 3820, Apr. 2023.

[Koigerov-22] Koigerov, Aleksey S., "Modern Physical-Mathematical Models and Methods for Design Surface Acoustic Wave Devices: COM Based P-Matrices and FEM in COMSOL" *Mathematics,* vol. 10, no. 22, pp. 4353, Nov. 2022.

[Haghighi-23] Haghighi, S., Haghighatzadeh, A. and Attarzadeh, A., "Modeling of electronic spectra and optical responses of a laser-affected double GaAsSb/GaAs parabolic quantum well using COMSOL multiphysics: the role of position-dependent effective mass and the static electric field", *Opt Quant Electron*, vol. 55, pp. 1052, Nov. 2023.

[Dávalos-Guzmán-23] J. Dávalos-Guzmán, J. L. Chavez-Hurtado and Z. Brito-Brito, "Neural Network Learning Techniques Comparison for a Multiphysics Second Order Low-Pass Filter," *2023 IEEE MTT-S Latin America Microwave Conference (LAMC)*, San José, Costa Rica, pp. 102-104, 2023.

[Nakilcioğlu-22] Nakilcioğlu, E., Rizvanolli, A. and Rendel, O., "Workload forecasting of a logistic node using Bayesian neural networks," *Chapters from the Proceedings of the Hamburg International Conference of Logistics (HICL)*, in: Kersten, W., Jahn, C., Blecker, T., Ringle, C. M. (ed.), *Changing Tides: The New Role of Resilience and Sustainability in Logistics and Supply Chain Management – Innovative Approaches for the Shift to a New* , vol. 33, pp. 237-264, Hamburg University of Technology (TUHH), Institute of Business Logistics and General Management, 2022.

[Pugalenthi-22] K. Pugalenthi, H. Park, S. Hussain, and N. Raghavan, "Remaining useful life prediction of lithium-ion batteries using Neural Networks with adaptive Bayesian learning," *Sensors*, vol. 22, no. 10, pp. 3803, May 2022.

[Zeng-23] Zeng, X., Yang, Z., Zhang, L., Tang, X., Zeng, Z., and Liu, Z. "Safety Verification of Nonlinear Systems with Bayesian Neural Network Controllers" in *Proceedings of the AAAI Conference on Artificial Intelligence*, vol. 37, no. 12, pp. 15278-15286, Jun. 2023.

[Liu-22] Y. Liu *et al*., "An Efficient Method for Antenna Design Based on a Self-Adaptive Bayesian Neural Network-Assisted Global Optimization Technique," in *IEEE Transactions on Antennas and Propagation*, vol. 70, no. 12, pp. 11375-11388, Dec. 2022.

[Aliqab-23] Aliqab, K., Sohaib, M.A., Ali, F., Armghan, A., Alsharari, M., "Employment of Self-Adaptive Bayesian Neural Network for Systematic Antenna Design: Improving Wireless Networks Functionalities", *Micromachines*, vol. 14, no. 3, pp. 594, Mar. 2023.

[Dávalos-Guzmán-24] Jorge Dávalos-Guzmán, José L. Chávez-Hurtado and, Zabdiel Brito-Brito, "A Bayesian Neural Network Approach with Latin Hypercube Sampling for Electromagnetic Characterization of Synthetical LC Circuits," Internal Report *PhDEngScITESO-XX-XX-R (CAECAS-XX-XX-R)*, ITESO, Tlaquepaque, Mexico, Feb. 2024.

[Güneş-17] F. Güneş, P. Mahouti, S. Demirel, M. A. Belen, and A. Uluslu, "Cost-effective GRNN-based modeling of microwave transistors with a reduced number of measurements," *International*

Journal of Numerical Modelling: Electronic Networks, Devices and Fields, vol. 30, no. 3-4, Aug. 2017.

[Borisut-20] P. Borisut and A. Nuchitprasittichai, "Process Configuration Studies of Methanol Production via Carbon Dioxide Hydrogenation: Process Simulation-Based Optimization Using Artificial Neural Networks," *Energies*, vol. 13, no. 24, 6608, Dec. 2020.

[Dávalos-Guzmán-23] J. Dávalos-Guzmán, J. L. Chavez-Hurtado and Z. Brito-Brito, "Neural Network Learning Techniques Comparison for a Multiphysics Second Order Low-Pass Filter," *2023 IEEE MTT-S Latin America Microwave Conference (LAMC)*, pp. 102-104, San José, Costa Rica, 2023.

[Li-17] S. Li, S. Zhang, C. Jiang, J. R. Mayor, T. G. Habetler and R. G. Harley, "A fast control-integrated and multiphysics-based multi-objective design optimization of switched reluctance machines," *2017 IEEE Energy Conversion Congress and Exposition (ECCE)*, pp. 730-737, Cincinnati, USA, 2017.

[Krishna-08] Krishna, K. Sri Rama, J. Lakshmi Narayana, and L. Pratap Reddy. "ANN models for microstrip line synthesis and analysis." *Int. J. Elect. Syst. Sci. Eng 1*, no. 3, pp. 196-200, 2008.

[Uluslu-23] A. Uluslu, "Application of Artificial Neural Network Base Enhanced MLP Model for Scattering Parameter Prediction of Dual-band Helical Antenna", *ACES Journal*, vol. 38, no. 05, pp. 316–324, Sep. 2023.

[Calik-19] N. Calik, M. A. Belen, and P. Mahouti, "Deep learning base modified MLP model for precise scattering parameter prediction of capacitive feed antenna," *International Journal of Numerical Modelling: Electronic Networks, Devices and Fields*, vol. 33, no. 2, Sep. 2019.

[Unger-11] J. F. Unger and C. Könke, "An inverse parameter identification procedure assessing the quality of the estimates using Bayesian neural networks," *Applied Soft Computing,* vol. 11, no. 4, pp. 3357-3367, Jun. 2011.

[Wang-23] Wang, J.; Ji, H.; Qi, A.; Liu, Y.; Lin, L.; Wu, X.; Ni, J. "Intelligent Optimization Design of a Phononic Crystal Air-Coupled Ultrasound Transducer", *Materials 2023,* 16, no. 17:5812, 2023.

[Yangfan-20] Yangfan Qin, Hao Jiang, Yanjun Cong, Guangyao Li, Lin Qi & Junjia Cui (2021) Rivet die design and optimization for electromagnetic riveting of aluminium alloy joints, *Engineering Optimization*, vol. 53, no. 5, pp. 770-788, Apr. 2020.

[Mahouti-19] P. Mahouti, "Design optimization of a pattern reconfigurable microstrip antenna using differential evolution and 3D EM simulation-based neural network model," *International Journal of RF and Microwave Computer-Aided Engineering*, vol. 29, no. 8, Aug. 2019.

[Çalik-21] N. Çalik, M. A. Belen, P. Mahouti, and S. Koziel, "Accurate modeling of frequency selective surfaces using fully-connected regression model with automated architecture determination and parameter selection based on bayesian optimization," *IEEE Access*, vol. 9, pp. 38396-38410, 2021.

[MacKay-92] D. J. C. MacKay, "Bayesian interpolation," *Neural Computation*, vol. 4, no. 3, pp. 415-447, May 1992.

[Mahouti-14] P. Mahouti, F. Güneş, S. Demirel, A. Uluslu, and M. A. Belen, "Efficient scattering parameter modeling of a microwave transistor using generalized regression neural network," *20th International Conference on Microwaves, Radar and Wireless Communications (MIKON)*, Gdansk, Poland, pp. 1-4, June 2014.

Author Index

Subject Index

T

V

W

Y